Australian Government
Department of Defence
Defence Science and
Technology Organisation

The Effect of Weld Penetration on Blast Performance of Welded Panels

Emily Frain and Len Davidson

Maritime Division
Defence Science and Technology Organisation

DSTO-TR-3017

ABSTRACT

A modified explosion bulge test method was used demonstrate the difference in performance of full-penetration (nominally 100%) welds and partial-penetration (nominally 70%) welds under blast loading. The welded coupons consisted of armour steel plate, Bisalloy BisPlate High Hardness Armour steel, welded to Bisalloy BisPlate80 steel with an austenitic filler material, TETRA S 20 9 3-G . If was found that full-penetration welds will withstand, without cracking, closer blasts, and correspondingly greater blast loading, than partial penetration welds. However, there may be some critical length and size dimensions of the incomplete penetration for which the blast performance of the welded panel is not adversely affected.

RELEASE LIMITATION

Approved for Public Release

Published by

Maritime Division
DSTO Defence Science and Technology Organisation
506 Lorimer St
Fishermans Bend, Victoria 3207 Australia

Telephone: 1300 333 362
Fax: (03) 9626 7999

© Commonwealth of Australia 2014
AR-016-068
August 2014

APPROVED FOR PUBLIC RELEASE

The Effect of Weld Penetration on Blast Performance of Welded Panels

Executive Summary

If an armoured vehicle is subjected to explosive blast loading, such as, detonation of a mine or an Improvised Explosive Device (IED), the blast has the potential to cause extensive damage to the vehicle and serious injury to the occupants. The ingress of high velocity detonation products into the vehicle introduces a significant potential for occupant injury. Hull weld rupture provides an opportunity for the ingress of these detonation products, thus the blast resistance of welds to rupture is of critical interest. This naturally raises questions regarding how weld defects will affect the blast resistance of those welds. The work reported here is concerned with the degree to which lengths of partial penetration along a hull weld may have a detrimental effect on the structures blast resistance.

The testing outlined in this report demonstrates the difference in performance of full-penetration (nominally 100%) welds compared to partial-penetration (nominally 70%) welds under blast loading. A modified explosion bulge test was used to assess the deformation and cracking of welded coupons under explosive loading. The coupons consisted of Bisalloy BisPlate High Hardness Armour (BisPlate HHA) welded to Bisalloy BisPlate80 (BisPlate80) steel with an austenitic filler material.

As anticipated, the plate deformations generally increased with decreasing explosive stand-off distance for both welding conditions. However, the full-penetration welded coupons were found to accommodate approximately 50% more deformation before experiencing cracking. This is partly due to the 35% reduction in load bearing cross sectional area caused by a combination of the unfused plate at the root of the partial-penetration welds and the smaller weld reinforcement size in the partial penetration welds. The other factor contributing to the reduced blast resistance of the partial-penetration coupons is the crack-like flaw found at the root of the welds which acts as a stress concentrator and is a favourable site for crack growth. Cracking in the partial-penetration coupons always occurred in the weld zone and included the unfused area of plate that is the crack-like flaw.

In contrast, the greater load bearing cross-section of the full-penetration coupons allowed these coupons to avoid strain localisation and associated tensile tearing in the weld zone and instead to continue deforming (albeit asymmetrically due to the differing material strengths) until cracking was initiated in the BisPlate80 plate material at the apex of the bulge (outside the weld zone).

These results demonstrate that the full penetration welds will withstand, without cracking, closer blasts, and correspondingly greater blast loading, than partial

penetration welds. Furthermore, the survivability of a welded vehicle could potentially be enhanced by incorporating full penetration welding requirements.

The tests showed that there may be some critical length and size dimensions of partial-penetration for which the blast performance of the weld is not adversely affected. Knowledge of this critical size could potentially be used for weld specification purposes in the future.

Authors

Emily Frain
Maritime Division

Emily Frain completed a combined Bachelor of Engineering and Bachelor of Science (Hons) with Physics and, Mechanical and Materials Systems majors at the Australian National University in 2008. Since 2009 she has worked as a graduate engineer/scientist in the Armour Mechanics and Vehicle Survivability Group of the Maritime Platforms Division of DSTO. In this time she has contributed to full scale vehicle survivability and blast trials as well as battle damage assessments of land vehicles.

Len Davidson
Maritime Division

Len Davidson is the Head of the Structural Materials and Fabrication Group of the Maritime Division of DSTO. He received a BSc (Hons) from the University of New Brunswick in 1983 and a PhD from Monash University in 1989. Since joining DSTO in 1992 his research interests have included weld metal structure-property relationships for improved resistance to blast and to hydrogen induced cracking as well as remaining life assessments and life extension of defence platforms

This page is intentionally blank

Contents

1. INTRODUCTION **1**

2. AIM **2**

3. PROCEDURE **2**
3.1 Test Set-up **2**
3.2 Post Blast Deformation and Thinning Measurement **5**

4. TEST COUPONS **6**
4.1 Materials, Manufacture and Preparation **6**
4.2 Test Coupon Weld Characterisation **9**

5. RESULTS **14**
5.1 Coupon Deformation and Thinning **15**
5.2 Coupon Cracking Results **18**
5.2.1 Crack Location in Partial-penetration Coupons 20
5.2.2 Crack Location in Full-penetration Coupons 22
5.2.3 Crack Location in Nominally Full-penetration Coupons with Incomplete Penetration 24
5.3 Fracture Characteristics **25**
5.3.1 Partial-penetration Coupon 25
5.3.2 Full-penetration Coupon 27

6. DISCUSSION **28**

7. CONCLUSIONS **31**

8. FUTURE ANALYSIS **31**

ACKNOWLEDGEMENTS **32**

REFERENCES **33**

APPENDIX A: MANUFACTURER'S MATERIAL DATA SHEETS **34**
Plate Material Specifications **34**
Consumable Material Specifications **36**

APPENDIX B: QUANTITATIVE CHEMICAL ANALYSIS **38**

APPENDIX C: SEMI-QUANTITATIVE COMPOSITIONAL ANALYSIS OF A PARTIAL-PENETRATION AND FULL-PENETRATION COUPON 39

APPENDIX D: COUPON DEFORMATION 40

APPENDIX E: THINNING OF COUPONS WITH CRACKING 41

List of Abbreviations

Improvised Explosive Device	IED
Defence Science and Technology Organisation	DSTO
Explosion Bulge Test	EBT
High Hardness Armour	HHA
High Explosive Firing Chamber	HEFC
Heat Affected Zone	HAZ
Gas Metal Arc	GMA

This page is intentionally blank

1. Introduction

In most recent global conflicts Improvised Explosive Devices have presented armed forces with significant challenges. These relatively inexpensive devices are capable of causing significant damage to armoured vehicles, which are frequently constructed of welded metal plate. Rupture of a vehicle hull weld may allow the ingress of high velocity detonation products and other ejecta that could cause serious injury or death to occupants. The quality of a weld is expected to affect the blast performance of a vehicle hull.

Vehicles that are designed for blast resistance are often only required to meet fitness-for-purpose specifications demonstrated by means of a full-scale explosive test of a complete instrumented vehicle. However, welding is an inherently variable fabrication process and there exists the potential for undesirable discontinuities to be present in the structure of some vehicles.

Thus far there has been no testing to assess the risk posed by the presence of welding discontinuities, such as partial-penetration, in an armoured vehicle. The presence of incomplete or partial penetration along lengths of a welded vehicle has the potential to significantly reduce the blast resistance of the structure. Incomplete or partial-penetration, shown in Figure 1 (a), is where two opposing weld beads do not interpenetrate. In contrast, a full-penetration weld, shown in Figure 1 (b), will have interpenetration of the two opposing weld beads. Partial-penetration discontinuities can be detected using radiographic or ultrasonic inspection methods.

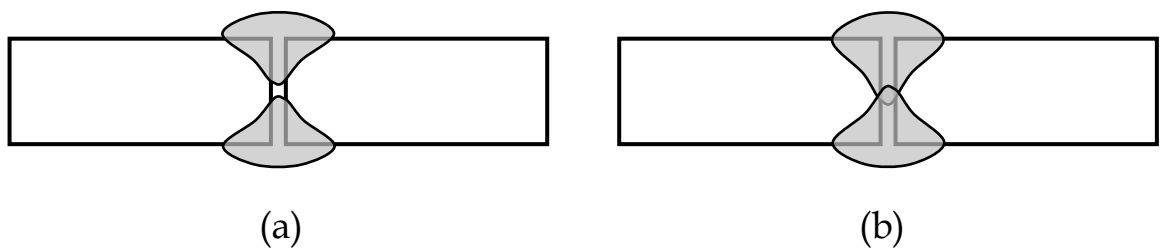

Figure 1: (a) A partial-penetration and (b) a full-penetration butt weld

Welded joints pose many technical challenges to an armoured vehicle manufacturer who must balance the requirements of blast and ballistic protection, structural strength, fatigue resistance, unit mass and production cost.

The testing described in this report provides a greater understanding of how weld penetration influences the blast performance of welded joints between Bisplate HHA and Bisalloy80. This test configuration could be adapted to assess the effects of a number of different weld quality parameters on the blast resistance of a welded joints.

2. Aim

To determine whether incomplete weld penetration significantly degrades the blast resistance of plates of Bisalloy BisPlate80 steel welded to Bisalloy BisPlate High Hardness Armour (BisPlate HHA) steel.

3. Procedure

3.1 Test Set-up

The set-up for each blast test of this experiment closely resembles that of the Explosion Bulge Test (EBT) which was developed in 1950 and is used to investigate factors that determine the performance of weldments in response to blast loading [1, 2]. The EBT is used to assess both ferrous and non-ferrous materials, weld filler materials and welding procedures. In the past, the EBT set-up has been adopted to investigate the effect of weld defects under blast loading where overmatching weld filler materials were used in the weld, i.e. the yield strength of the weld consumable was greater than that of the parent plate [3, 4]. In the current work the weld metal was undermatched with regard to both the BisPlate80 and the BisPlate HHA, i.e. the yield strength of the weld consumable was less than that of both parent plates.

The welded coupons consisted of 8.5 mm nominal thickness, BisPlate HHA, welded to 8.0 mm nominal thickness BisPlate80 steel with an austenitic filler material, TETRA S 20 9 3-G. This selection of plate and filler materials is thought to be a reasonable representation of the materials that could be selected for use on an armoured vehicle and will be discussed further in section 4.

In an EBT a test coupon measuring 760 mm by 760 mm is placed on an annulus-shaped die to allow the test coupon to bulge as a result of loading generated by an explosive charge suspended above the coupon. A schematic of the EBT test configuration is shown in Figure 2. The bulged coupon is described as having a 'compression' side, the side facing the charge, and 'tension' side, the side facing the die, which follows the convention defined within the standard for explosion bulge testing [5]. However, as the applied loading often produces deflections that are greater than half the plate thickness it is more likely that the full thickness of the plate experiences tension. Nevertheless, the tension/compression nomenclature has been maintained in this report for consistency with the standard.

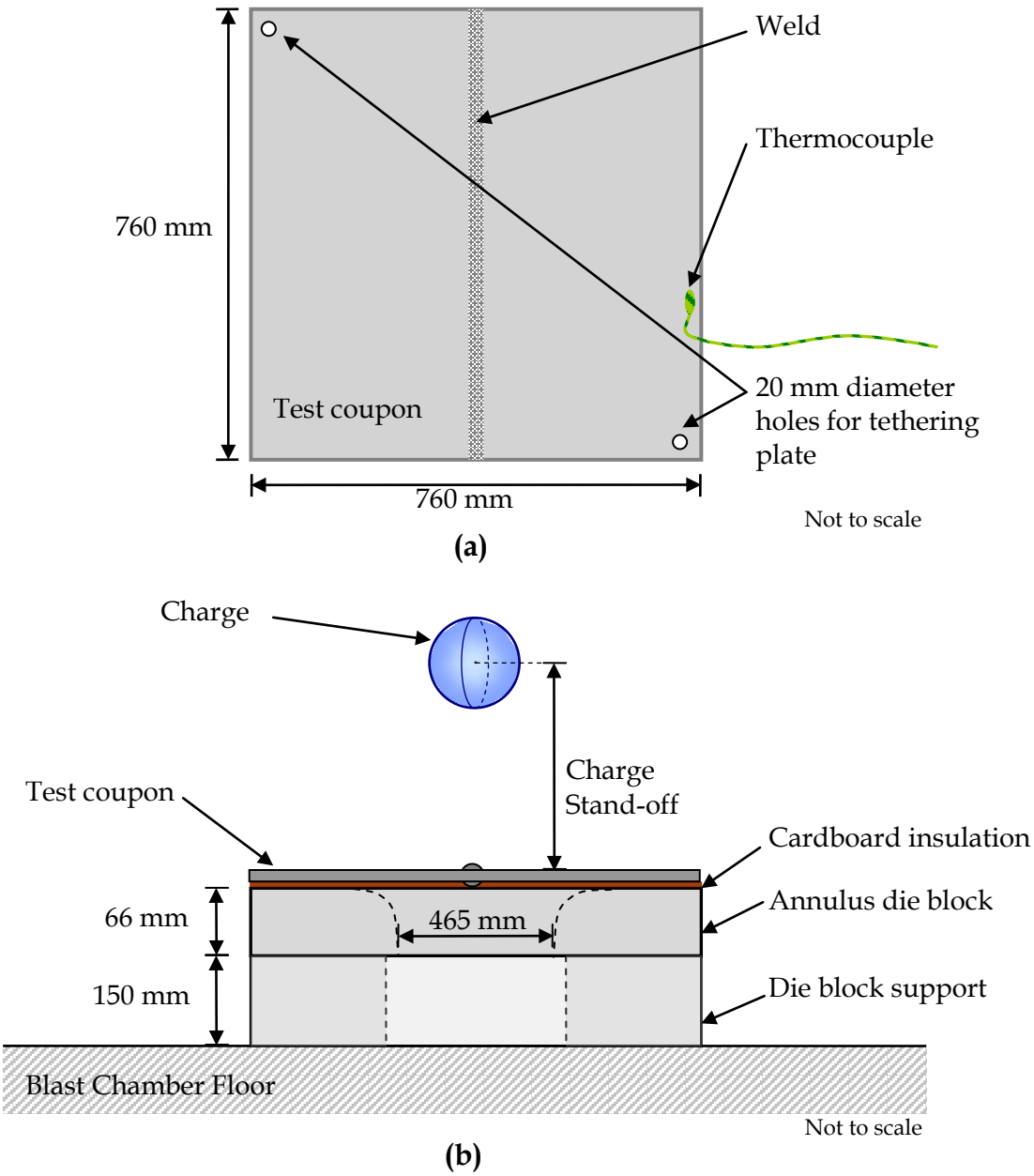

Figure 2: Schematic diagram of (a) a test plate showing plate dimensions, thermocouple location, weld and location of holes and (b) the test set-up immediately before each test.

In this series of tests the stand-off distance, defined as the distance between the compression surface of the test coupon and the centre of the charge, was the parameter varied — decreasing the stand-off resulted in more severe blast loading.

Tests were conducted in the 3 kg Explosion Chamber at the High Explosives Firing Complex (HEFC) at DSTO's Edinburgh site. A photograph of the test setup is shown in Figure 3.

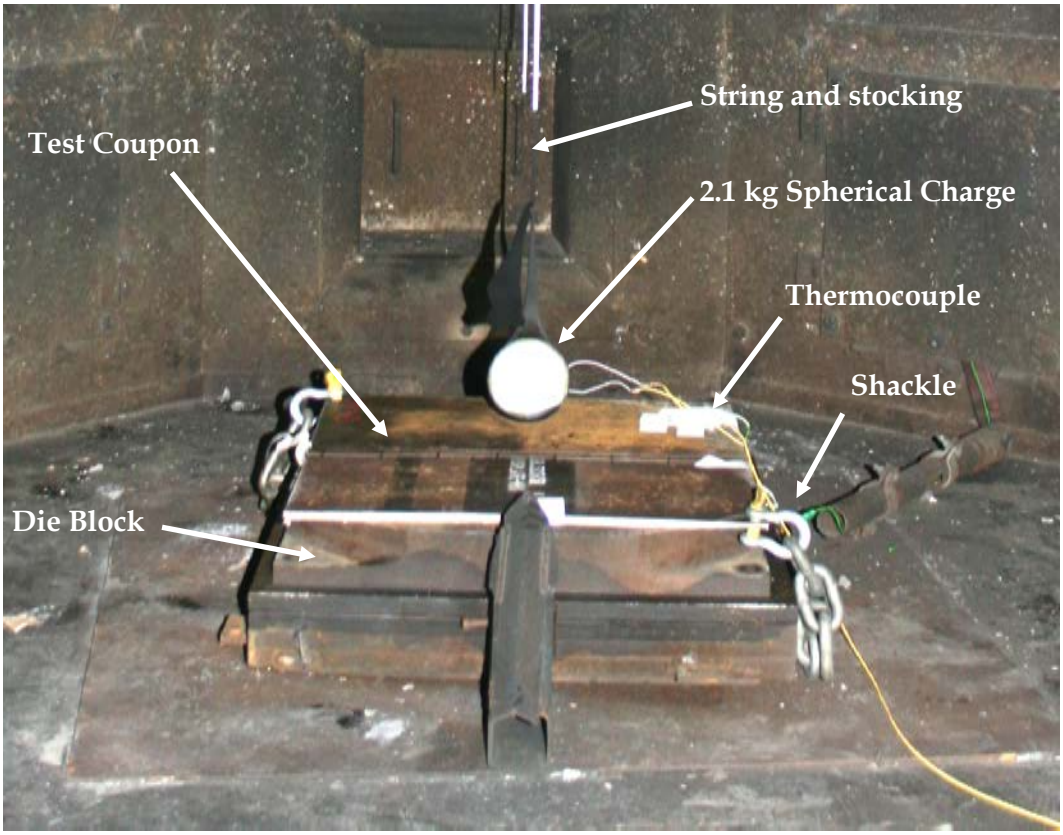

Figure 3: Experimental set-up in Blast Chamber

The coupon temperature for all tests was 0˚C. In each test a coupon was removed from a conditioning chamber, where it had been held for over twelve hours at a temperature not more than -5˚C, and was placed on the die block inside the firing chamber. The upper layer of insulating cardboard was removed and the coupon shackled to the die. The charge was suspended in a stocking from the ceiling of the chamber at the specified stand-off distance for the blast. The temperature of the coupon was monitored by a type 'k' thermocouple spot welded to the surface of the coupon. The thermocouple was connected to a National Instruments Compactdaq data acquisition system and was monitored from the HEFC control room. The charge was detonated once the temperature indicated by the thermocouple was 0˚C.

Sterjovski et al. [6] found that there will be a temperature gradient between the centre and the edge of the coupon as it warms for steel coupons of comparable size and thickness. Their results showed that the temperature difference between a thermocouple at the edge and a thermocouple at the centre of the plate did not exceed 4˚C (for a test plate with cardboard insulation between the plate and the die block) and that the temperature difference decreased as the plate temperature approached 0˚C [7]. From the available data it is unlikely that the edge of the plate will be more than 3˚C warmer than its centre.

A spherical charge was selected to achieve greater consistency in the shape of the explosive loading and to increase the potential for scalability and comparisons with future experimentation. The charge consisted of two high density polyethylene hemispheres packed with a combined mass of 2.100 ± 0.025 kg PE4 plastic explosive. The charge was initiated with an RP80 detonator positioned as shown in Figure 4.

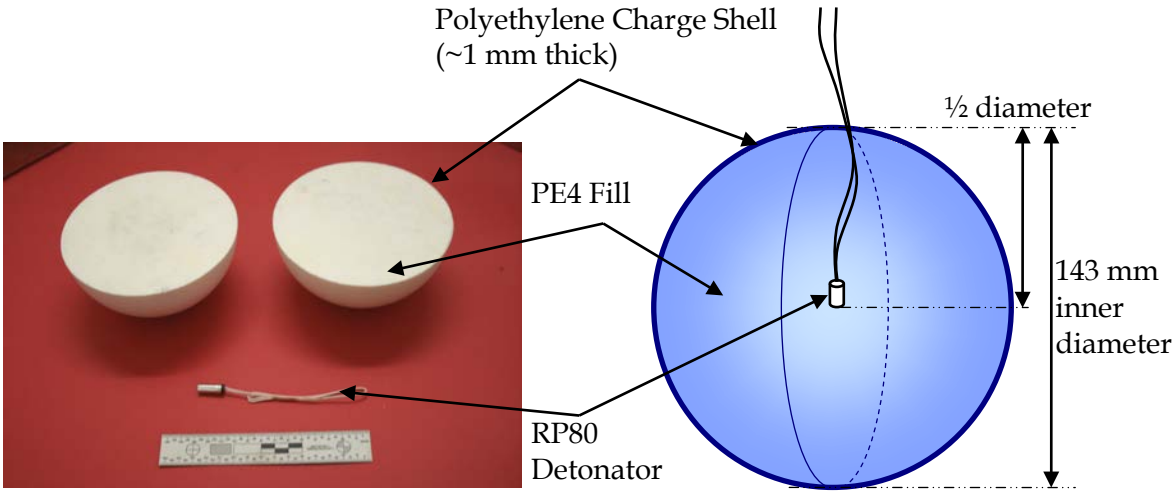

Figure 4: Charge configuration for all tests

The purpose of these tests was to identify a 'threshold' stand-off distance for coupon failure; that is, a stand-off distance above which the plate exhibited no cracking (no failure) and below which the coupon cracked (failure). The threshold stand-off distance at which failure occurred in welded coupons with partial-penetration was then compared to the threshold stand-off distance for failure of the full-penetration coupons.

3.2 Post Blast Deformation and Thinning Measurement

Post blast deformation was measured by placing a straight edge across a tested coupon, perpendicular to the weld bisecting the bulge, and using a caliper to measure the distance from the straight edge to the plate at intervals from the centreline of the weld, as shown in Figure 5.

Thinning of the coupons as a result of the blast was measured using an OLYMPUS Panametrics – NDT™ MG2-DL Ultrasonic Thickness Gauge. Nine measurements were taken as close as possible to the centre of the bulge and these were compared to six measurements taken at the periphery of the plate.

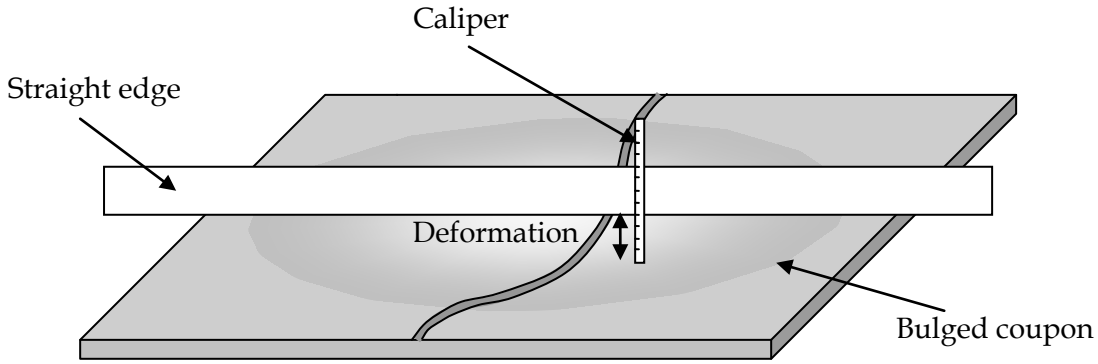

Figure 5: Method for measuring coupon deformation

4. Test Coupons

4.1 Materials, Manufacture and Preparation

BisPlate HHA is a quenched and tempered steel armour plate of high hardness, marketed for applications where light weight and resistance to ballistic projectiles is required. BisPlate80 is a quenched and tempered, high strength steel plate with excellent notch toughness. The microstructure of both plate materials is martensitic. Salient material properties are listed in Table 1 and the manufacturer's data sheet for each is contained in Appendix A.

Table 1: Plate mechanical properties (from Appendix A)

Material		Thickness (mm)	0.2% Proof Stress (MPa)	Tensile Strength (MPa)	Elongation in 50mm gauge length	Hardness
BisPlate80	(min)	8.0	690[1]	790-930[1]	18%[1]	
	(typical)		750	830	26%	255 HB
BisPlate HHA (typical)		8.5	1400	1640	14%	500 HB

Full quantitative chemical analysis of the two plate materials was conducted using inductively coupled plasma atomic emission spectroscopy. The results, included in Appendix B, are consistent with the manufacturer's specifications with the exception of marginally higher sulphur content in the BisPlate HHA.

The hardness of the two plate materials was measured using a King Brinell portable hardness indenter. The measured hardness of the BisPlate80 and the BisPlate HHA used in this test series was 291 Brinell (HBW/10/3000) and 514 Brinell (HBW/10/3000), respectively. The measured BisPlate80 hardness was greater than the typical hardness provided in the material specification.

[1] Depends on plate thickness

TETRA S 20 9 3-G is an austenitic filler material often selected for welding high strength armour steels to control hydrogen induced cold cracking. Hydrogen induced cold cracking occurs in welding as a result of the combined presence of tensile residual stresses, a susceptible microstructure and hydrogen absorption during the welding process [8]. Hydrogen has a higher solubility and lower diffusivity in austenite than in ferrite, therefore the hydrogen tends to remain in the weld metal, which is austenitic, rather than diffusing into the Heat Affected Zone (HAZ) and causing hydrogen induced cracking [9, 10].

In this study, the yield strength of the all-weld metal is lower than both plate materials, however the elongation is greater. Material properties of the consumable are listed in Table 2 and the manufacturer's data sheet is contained in Appendix A.

Table 2: TETRA S 20 9 3-G Weld consumable mechanical properties (from Appendix A)

TETRA S 20 9 3-G	0.2%Proof Stress (MPa)	Tensile Strength (MPa)	Elongation
Minimum	150	620	20%
Typical	530	710	30%

The test coupons consisted of a 385 x 765 x 8 mm BisPlate80 plate joined to a 385 x 760 x 8.5 mm BisPlate HHA plate. The plates were oxy-acetylene cut, followed by a machined edge preparation, with the major axis parallel to the rolling directions specified. The edge preparation removed the heat affected region imparted by the oxy-acetylene cutting process.

The plates were joined to each other along the major axis with a Gas Metal Arc (GMA) welding process using a Fronius TransPuls Synergic 5000 CMT machine guided by an ABB programmable robot as shown in Figure 6. The welding robot was used to maximise consistency between the welded coupons. Table 3 contains information regarding the welding procedure used to manufacture the coupons and the edge preparation is shown in Figure 7.

Table 3: Welding Procedure

Consumable:	1.2 mm diameter TETRA S 20 9 3-G
Shielding gas:	Argon
Preheat:	None
Run off/ run on plates:	Yes
Edge Preparation:	double bevel-groove and tee edge (bevel on the BisPlate80)

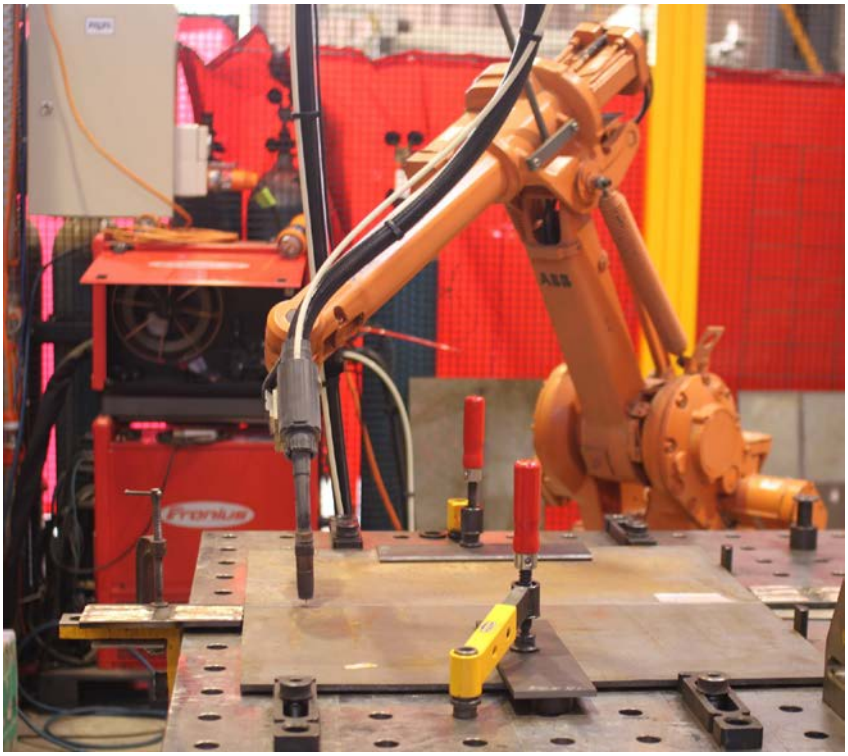

Figure 6: ABB robot and TransPuls Synergic 5000 CMT machine in position to conduct welding operation

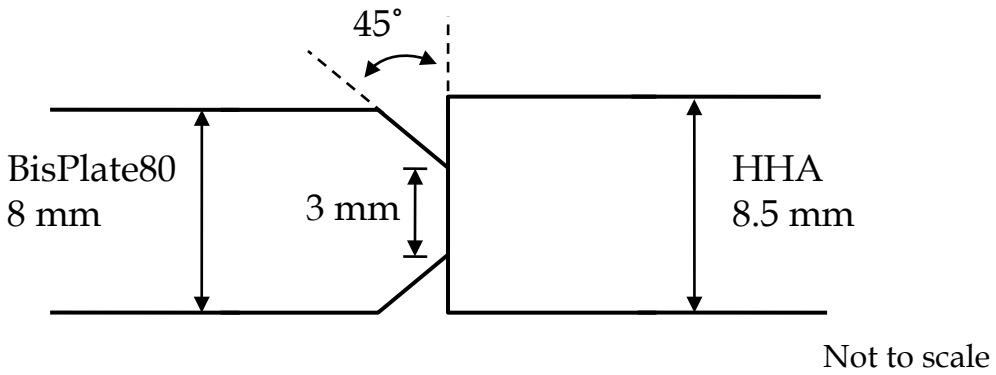

Figure 7: Edge preparation for GMA welding process

A total of 25 coupons were welded, 15 with parameters to achieve partial (approximately 70%) penetration and 10 with welding parameters to achieve full (100%) penetration. The welding parameters are listed in Table 4 and micrographs of the two weld conditions are shown in Figure 8. The estimated heat input is approximately 800 J/mm for the full-penetration condition and 780 J/mm for the partial-penetration condition.

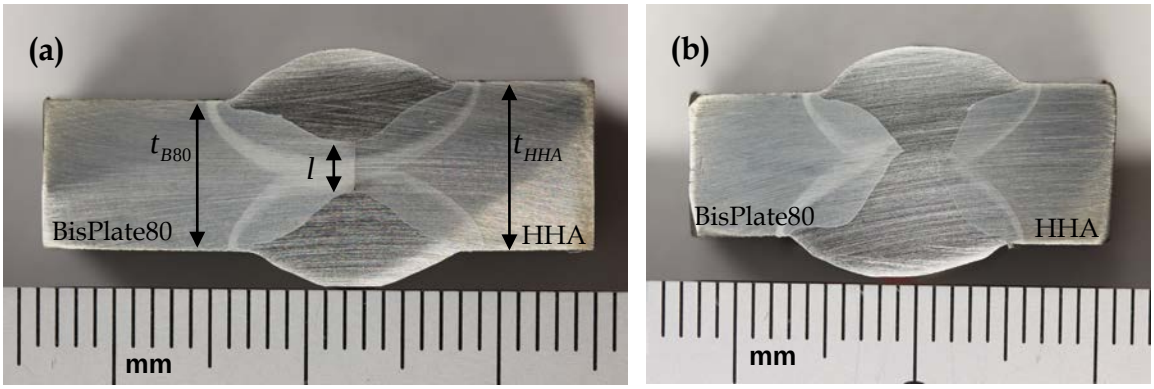

Figure 8: Micrographs showing (a) the partial (~70%) penetration weld and (b) the full (100%) penetration weld, where t_{B80}, t_{HHA} and l are the thickness of the BisPlate80, BisPlate HHA and the un-fused portion of the edge, respectively.

Table 4: Welding Parameters

Coupon type	Pass #	Current (A)	Voltage (V)	Travel Speed (mm/min)	Wire Feed Speed (m/s)	Polarity
Full-penetration	Pass 1	215	24.7	400	8	DC+
	Pass 2	217	24.7	400	8	DC+
Partial-penetration	Pass 1	298	26	600	14.2	DC+
	Pass 2	302	26	600	14.2	DC+

The coupons, once welded, measured approximately 760 mm x 760 mm. Two 20 mm diameter holes were drilled in each test coupon (in opposing corners) to allow them to be loosely tethered to the floor during testing in order to minimise damage to the blast chamber ceiling. A 150 mm length of weld reinforcement was removed from the weld ends on the tension side of the plate using a milling machine . This was done to allow the plate to sit flat upon the die.

A type 'k' thermocouple was spot-welded on one side of the plate near one of the corners to allow the temperature of the test-plate to be monitored during test set-up. The test plates were insulated with 5 mm thick cardboard and placed in the conditioning chamber. The purpose of the insulating cardboard was to reduce the heating rate of the test coupons after they were removed from the conditioning chamber and to thermally insulate the test coupon from the die.

4.2 Test Coupon Weld Characterisation

Welding is an inherently variable process and while robotic welding provides better control of weld quality there is still variation from run to run. The specified amounts of penetration for the two welding conditions were 70% and 100% penetration. The

percentage penetration was measured from the micrographs shown in Figure 8 and calculated using Equation 1.

$$\%Penetration = \frac{0.5(t_{B80} + t_{HHA}) - l}{0.5(t_{B80} + t_{HHA})} \times 100 \qquad \textit{Equation 1}$$

Where t_{B80}, t_{HHA} and l are measured as indicated in Figure 8.

The percentage penetration for the welds shown in Figure 8 (a) and (b) were 69% and 100%, respectively. The measured penetration of the partial-penetration coupons ranged from 63% to 69%.

There was distortion in the coupons as a result of the welding process. The largest measured deviation from flat was 4˚. In all tests the side of the plate with the obtuse angle (<180˚, >90˚) was positioned facing away from the die, resulting in this side being referred to as the compression side.

Each welded coupon was radiographed for an assessment of the discontinuities. The discontinuity severity grading system of MIL-STD-1894B [11] ranges from standard 1, which represents a high-quality weld, to standard 5, indicative of a poor-quality weld. With respect to porosity, slag and similar discontinuities, all coupons met standard 1 of this standard.

The radiographs of the partial-penetration coupons exhibited discontinuity indications consistent with incomplete penetration, as expected. Eight of the ten specified full-penetration coupons contained some minor incomplete penetration indications, with lengths less than 15 mm. Two of the ten specified full-penetration coupons contained indications of incomplete penetration. The lengths of the indications were 166 mm (coupon 100-02) and 210 mm (coupon 100-04).

Coupons 100-02 and 100-04 represent a less severe incomplete penetration condition than the specified partial-penetration coupons. The metallographic sections in Figure 9, taken after testing, show that the size of the incomplete penetration in the through thickness direction is approximately 1 mm, or a 90% penetration condition, for both coupons. These two plates were set aside until testing had established the threshold stand-off distance below which the full-penetration coupons exhibited cracking. Coupons 100-02 and 100-04 were then tested at that threshold stand-off distance in order to investigate the effect of threshold loading on a less severe incomplete penetration condition.

(a)

(b)

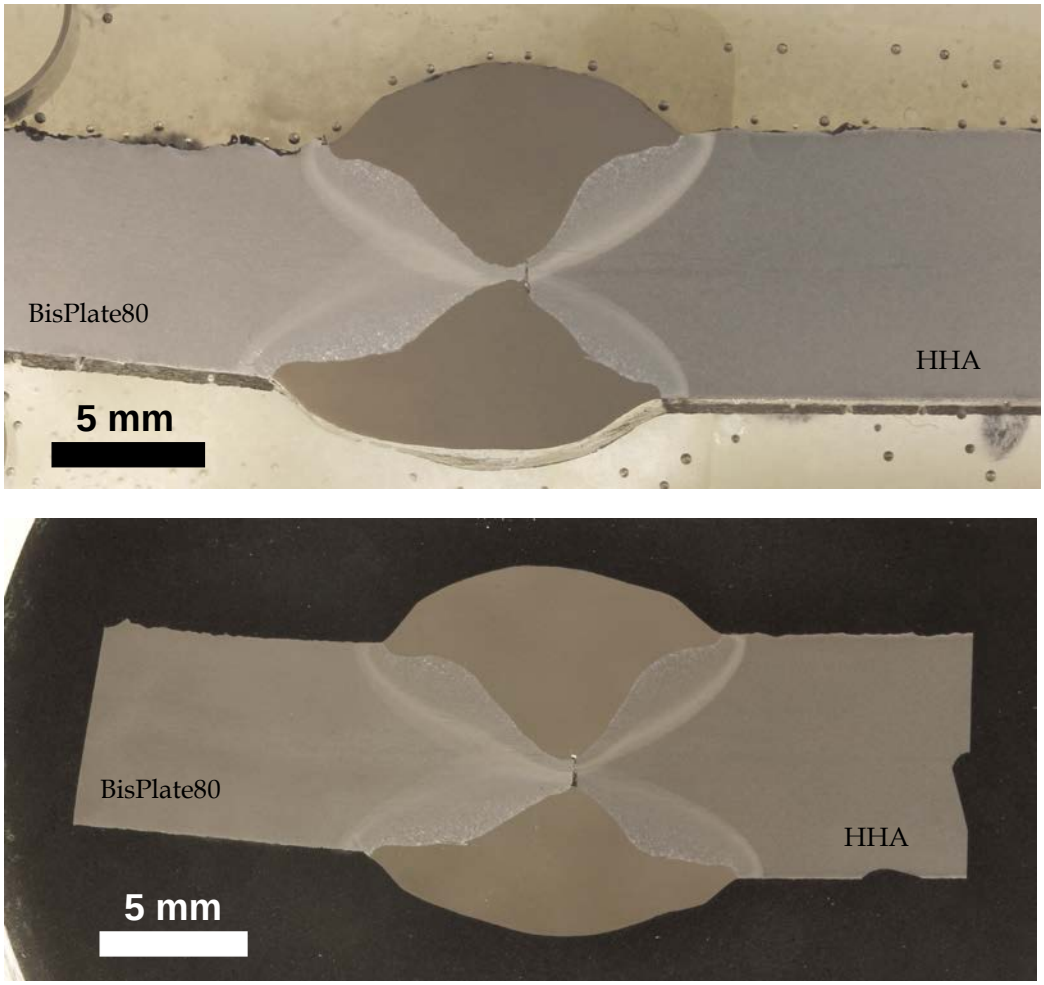

Figure 9: Polished and etched section of coupon labelled (a) 100-02 and (b) 100-04 showing less pronounced partial-penetration (~90% penetration).

It was found that the majority of coupons (both full and partial-penetration) exhibited features attributed to solidification cracking at the end of the weld run. However, because the solidification cracking was located at the plate edge where the loading would be lowest, they were considered inconsequential to the outcomes of the blast testing.

The area of weld reinforcement of the partial-penetration weld shown in Figure 8 (a) and the full-penetration weld shown in Figure 8 (b) were measured and the results are listed in Table 5.

Table 5: Area of Weld Reinforcement

	Area of reinforcement (mm^2)	
	1st Pass	2nd Pass
Partial-penetration	13.7	16.7
Full-penetration	17.7	17.1

A hardness traverse was performed across a mounted and polished section of both a partial-penetration and a full-penetration coupon. A Vickers hardness indenter with a 10 kg load was used for the hardness tests. The traverse was taken approximately 500 µm from the plate surface through the first pass, as shown in Figure 10 for the full-penetration coupon. These results have been plotted in Figure 11.

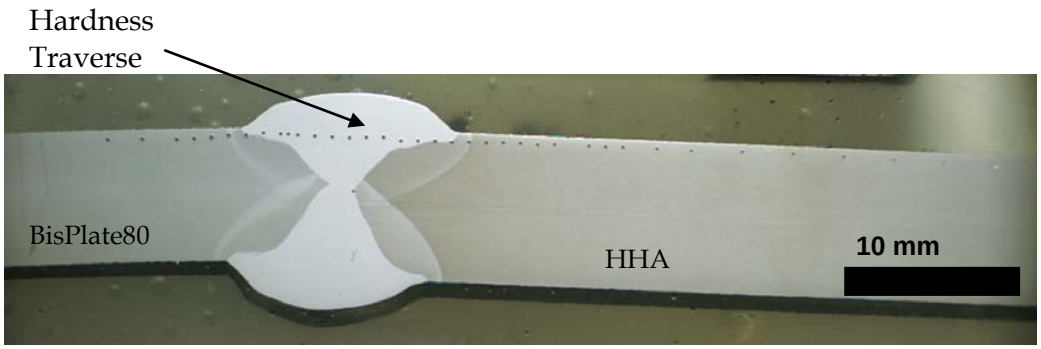

(a)

(b)

Figure 10: Hardness traverse across a section of (a) a full-penetration test coupon and (b) a partial-penetration test coupon.

The hardness traverses plotted in Figure 11 show that the weld hardness profile of the test coupons is reasonably consistent between the two welding conditions. The measured hardness of the weld material ranged between 382HV and 442HV.

The BisPlate80 HAZ extends approximately 4 to 6 mm from the fusion boundary, beyond which the BisPlate80 hardness values plateau at approximately 300HV. The hardness traverse values progressing from the fusion boundary into the BisPlate HHA plateau at approximately 520HV approximately 20 mm from the fusion boundary.

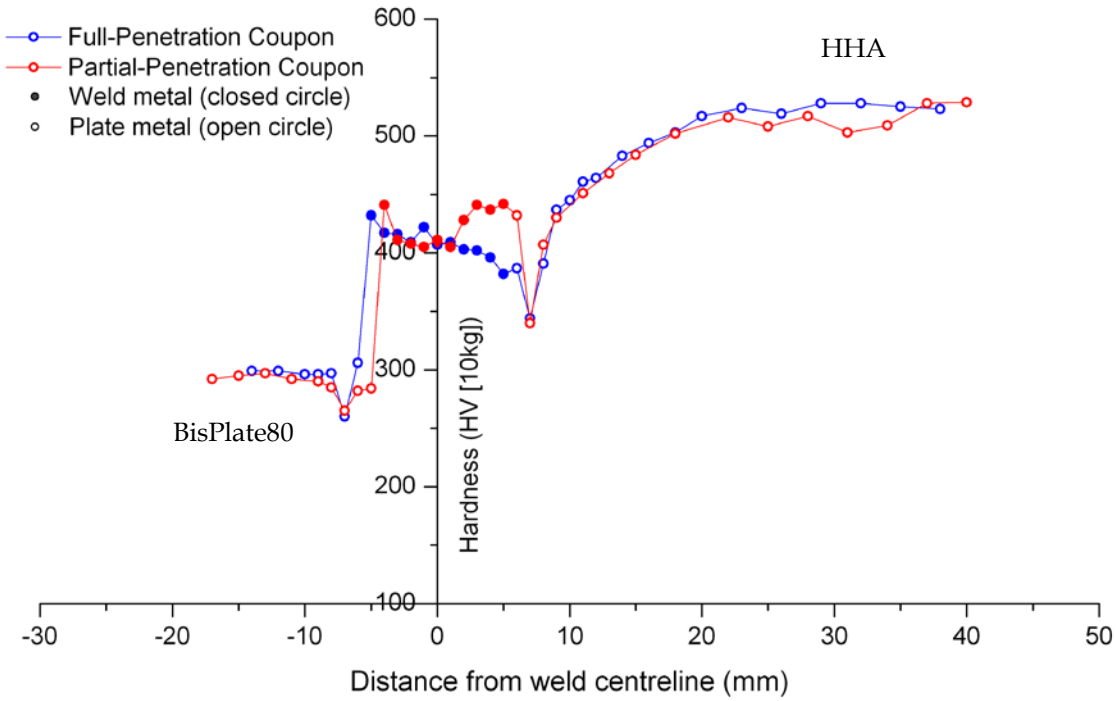

Figure 11: Hardness traverse across a partial-penetration (70%) and a full-penetration (100%) coupon.

Semi-quantitative[2] chemical analysis, using a scanning electron microscope coupled with energy dispersive spectroscopy, was performed on polished sections of a partial-penetration weld coupon and a full-penetration weld coupon. Two areas of each weld pass, the root and the reinforcement, were analysed along with both plate materials. The results of the semi-quantitative chemical analysis of the partial-penetration and full-penetration coupons are included in Appendix C.

[2] The semi-quantitative chemical analysis is a standardless surface microanalysis. The results are an approximation of the true composition of the spectrum analyses.

5. Results

Eighteen blast tests were conducted during the trial. The tests were conducted on ten partial-penetration coupons, six full-penetration coupons and two nominally full-penetration coupons that contained limited lengths of approximately 90% penetration weld. The response of the welded coupons to blast ranged from minimal detectable change, observed at a stand-off of 515 mm, to extreme deformation and extensive cracking in both the weld zone and the plate material at stand-off distances below 150 mm. The full spectrum of these responses is shown photographically in Appendix D and a categorical breakdown of observed coupon behaviour is shown diagrammatically in Figure 12.

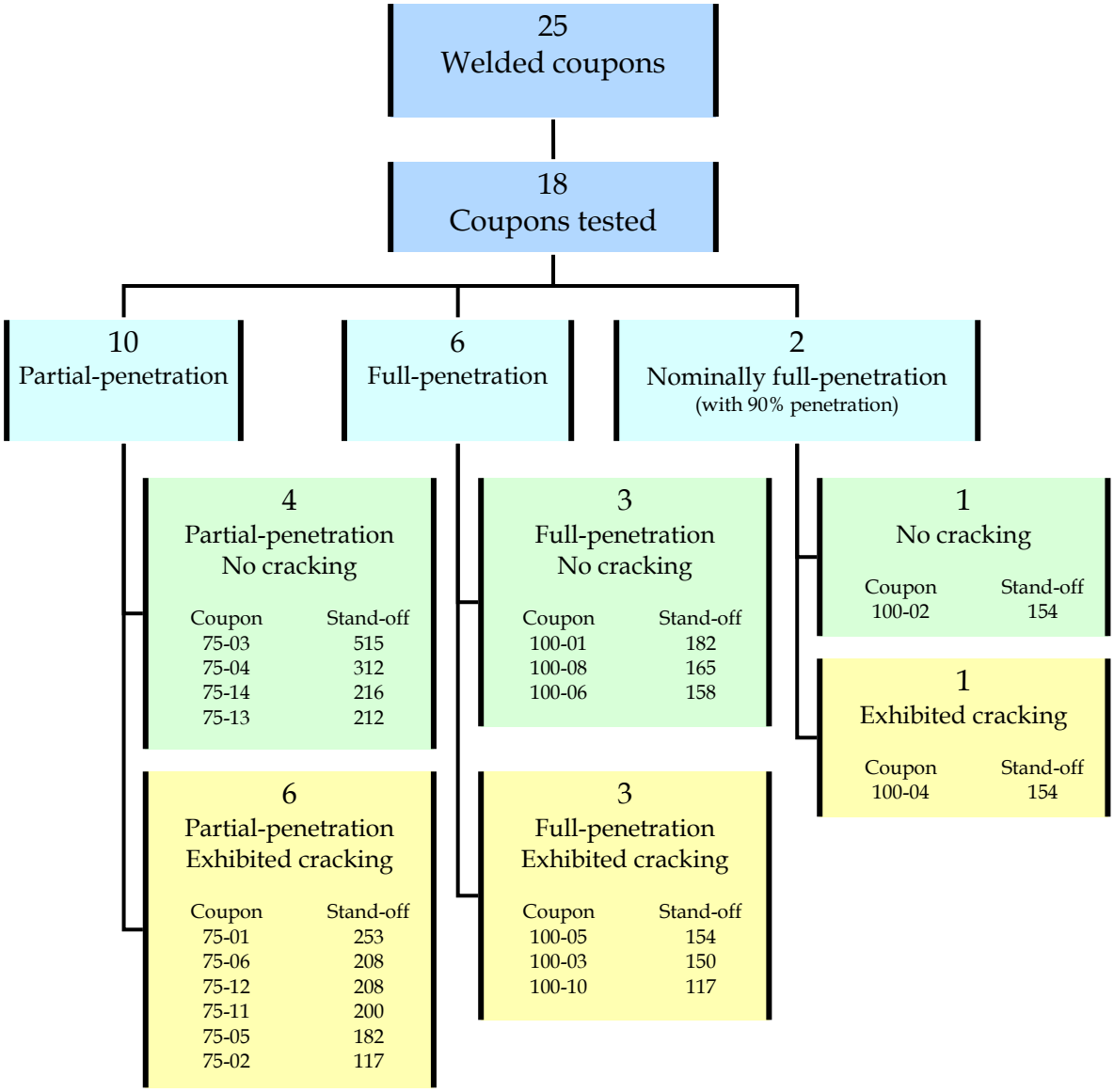

Figure 12: Categorical breakdown of observed coupon behaviour. Stand-off distances are expressed in millimetres

5.1 Coupon Deformation and Thinning

As anticipated, the plate deformation generally decreased with increasing stand-off distance for both welding conditions. This trend is illustrated in Appendix D. Coupon thinning and deformation measurements were most informative when taken on the seven uncracked coupons (four partial-penetration coupons and three full-penetration coupons) listed in Figure 12. The 90% penetration coupon that did not exhibit cracking, labelled 100-02, was treated as a separate case with an insufficient sample size to include in the thinning and deformation data.

Deformation measurements were made of the uncracked coupons across the weld centreline as described in Section 3.2. Figure 13 shows the deformation across the plate revealing the shape of the bulge. The deformation limit before coupon cracking for full-penetration coupons was approximately 31 mm greater than for partial-penetration coupons. This suggests that the full-penetration coupons were able to accommodate 50% more deformation before cracking. It can also be observed that the shape of the deformation is asymmetric with the BisPlate80 material exhibiting a more rounded bulge compared to the BisPlate HHA.

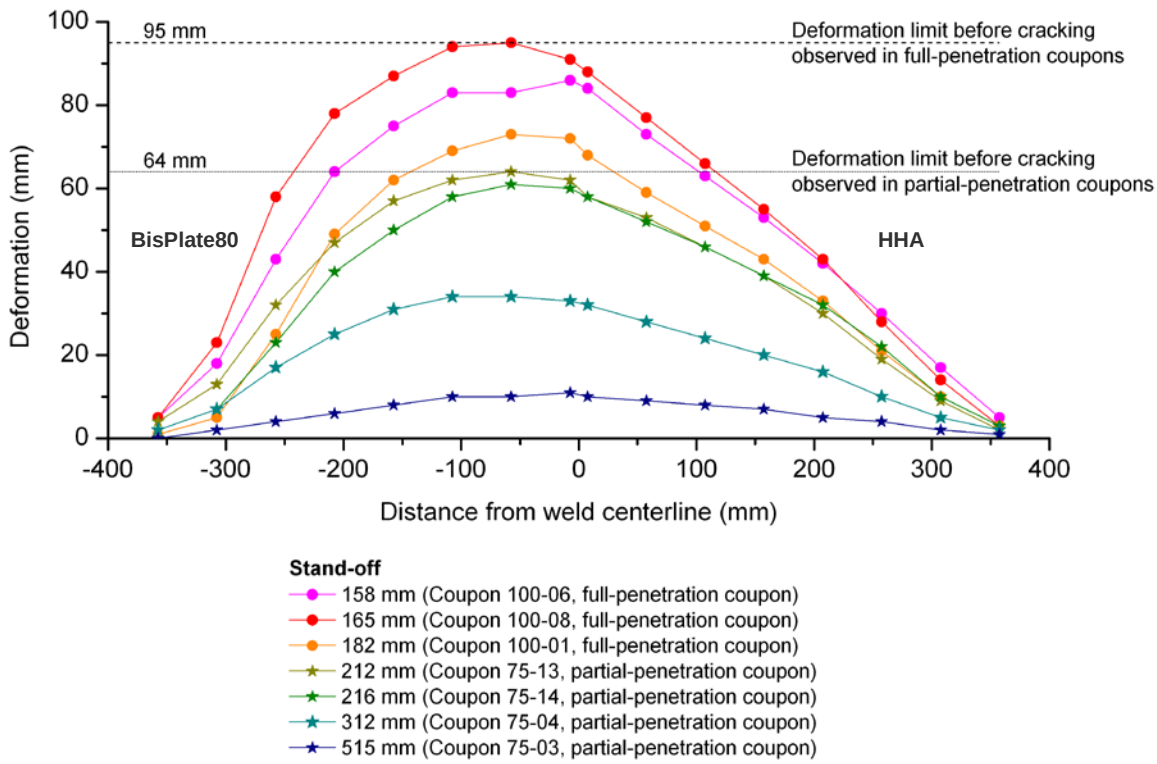

Figure 13: Centreline deformation of plates that did not exhibit cracking. The stand-off distance that corresponds to each test is specified in the legend. The negative distances denote BisPlate80 material whereas positive distances are BisPlateHHA; the weld centreline is the zero reference.

Figure 14 shows the measured deformation at the weld toe at the centre of the coupon as function of the stand-off, for both the BisPlate80 and the BisPlate HHA material. The plate deformation showed a trend of increasing deformation with decreasing stand-off distance. The results for the full-penetration coupons contain an apparent outlier to this trend (at 165 mm standoff). This is most likely to be an artefact of the deformation measurement technique and will be discussed in Section 6.

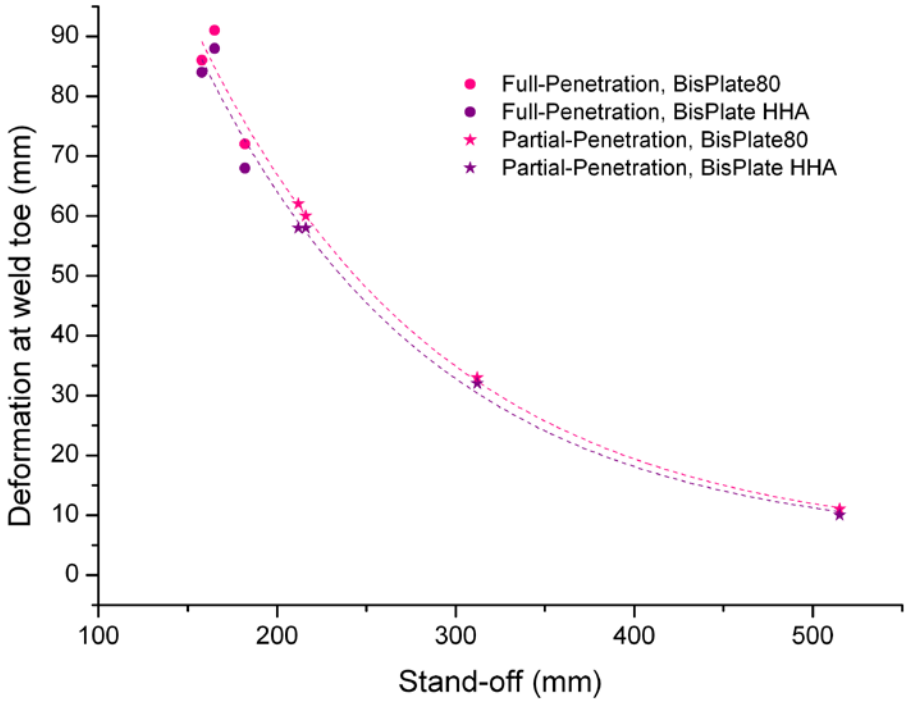

Figure 14: Bisplate80 (pink) and BisPlate HHA (purple) deformation measured at the centre of the un-cracked coupons at the weld toe. Lines have been drawn to guide the eye to the trend in the data.

Figure 15 shows the thinning that was measured on the full-penetration and partial-penetration coupons which did not exhibit cracking. The BisPlate80 material experienced greater thinning, in all but one test, in comparison to the BisPlate HHA material. The exception occurs when there is almost zero discernable thinning. This exception is most likely a result of the error in the thinning measurements and the variability of the plate thickness. A dashed line has been drawn to guide the eye to the trend where more thinning will occur at smaller charge stand-off distance.

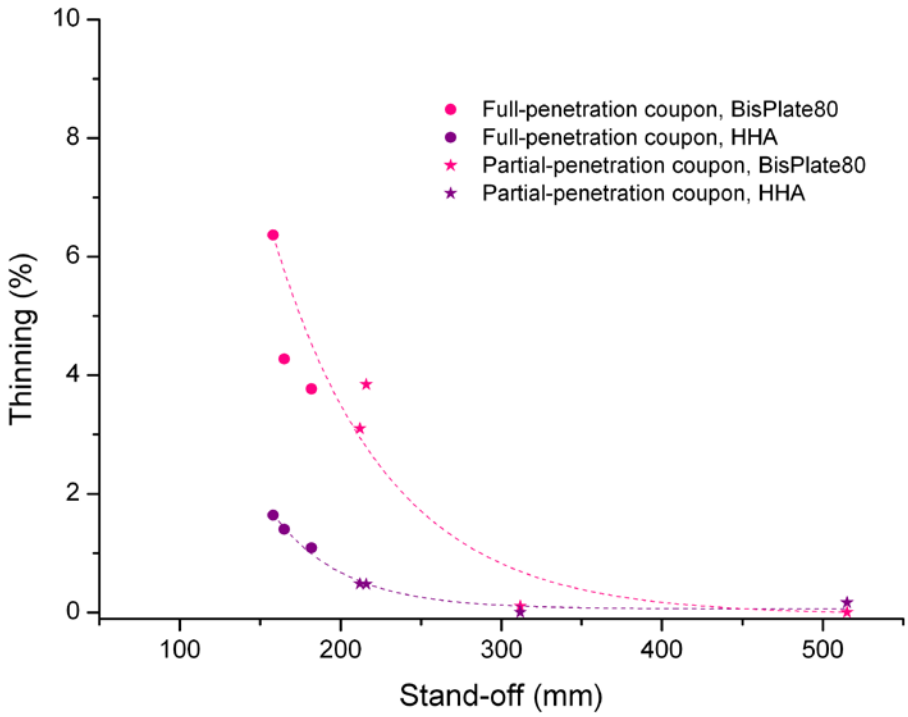

Figure 15: Thinning results from the coupons that did not exhibit cracking. Lines have been drawn to guide the eye to the trend in the data.

The cracked coupon thinning data (Appendix E) also shows a tendency for greater thinning in the lower yield strength BisPlate80 plate (typically 750 MPa) as compared to the higher yield strength BisPlate HHA (typically 1400 MPa). However, with respect to changing stand-off there is a large amount of scatter in the limited data and no apparent trend.

Error in the thinning measurements is always present as a result of the uneven surface topography created by the blast on the compression face of the plate. This is why an average of multiple thinning measurements was generated. The cross-section image of the compression side in Figure 16 shows the surface finish produced by close exposure to the blast. The compression surface is uneven and cratered with thickness variations that can be 0.25 mm or more.

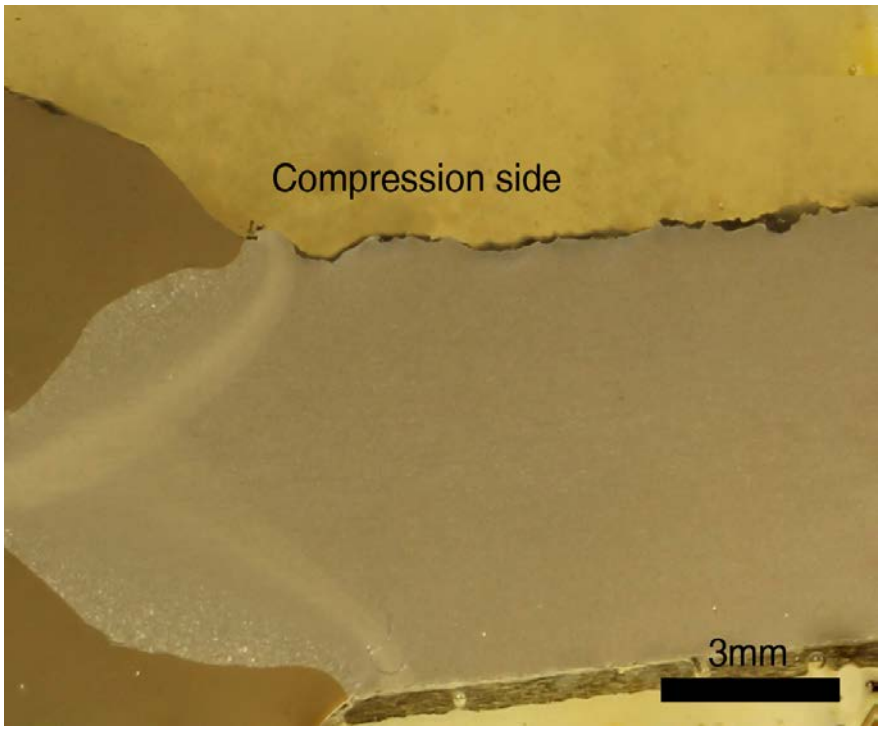

Figure 16: The uneven surface topography on the compression side of plate 100-02

5.2 Coupon Cracking Results

As stated previously the response of the coupons to the blast loading ranged from little discernable deformation to extensive cracking. Figure 12 contains a list of the coupons which exhibited cracking.

Figure 17 shows the length of cracking in the coupon, expressed as a percentage of coupon length, observed as a result of varying the stand-off distance between the charge and the coupon. Coupons 100-02 and 100-04, containing the unintended incomplete penetration defects, have been grouped by colour with the full-penetration data, albeit with an open symbol.

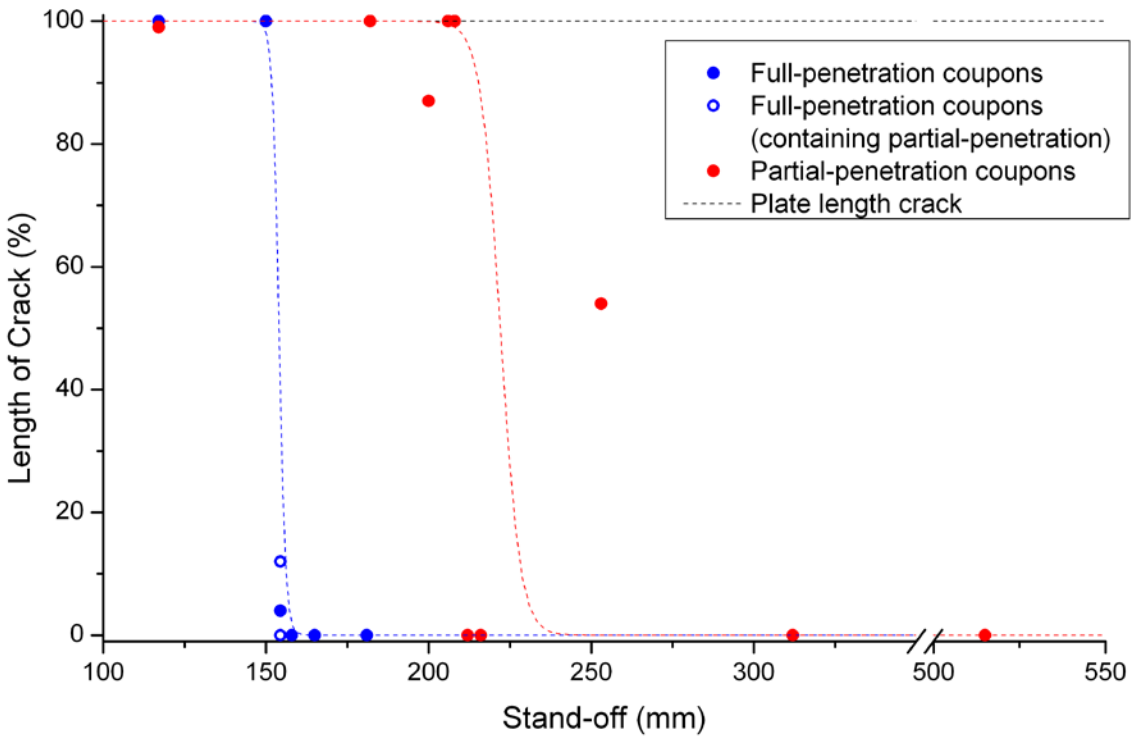

Figure 17: Longitudinal crack length results (expressed as a percentage of the coupon length) for coupons tested at different stand-off distances for the eighteen blast tests. The dashed lines have been drawn to guide the eye to the trends in the coupon behaviour and are not mathematical fits to the data.

The full-penetration data in Figure 17 shows that there is a distinct threshold stand-off, below which the coupon will exhibit cracking. The partial-penetration data shows a similar threshold, however there is more scatter in the results. Lines have been drawn in Figure 17 to guide the eye to the location of these thresholds but are not mathematical fits to the data. It is evident from these results that the stand-off distance at which failure occurs is greater for the partial-penetration weld condition.

Further illustrating the difference between the two welding conditions is the direct comparison between a partial-penetration coupon (75-05) and a full-penetration coupon (100-01), which were tested at the same stand-off distance of 182 mm (Figure 18). At this stand-off distance the partial-penetration coupon has completely failed through the weld zone, while the full-penetration coupon has deformed without cracking. The full-penetration coupons remained intact until the test stand-off distance was reduced to 154 mm.

The cracking in the partial-penetration coupons initiated and propagated in the weld zone in contrast to the cracking in the full-penetration coupons which initiated in the BisPlate80 material. This will be described further in the following two sections.

(a) **(b)**

Figure 18: A direct comparison of the blast resistance of; (a) a partial-penetration coupon and (b) a full-penetration coupon, where both were tested at a stand-off distance of 182 mm. The partial-penetration coupon failed completely whereas the full-penetration coupon did not exhibit cracking.

5.2.1 Crack Location in Partial-penetration Coupons

Six of the ten partial-penetration coupons exhibited cracking. Of these six, five showed cracking solely in the weld zone, that is, either through the weld metal or heat affected plate. The exception was the coupon tested at a stand-off of 117 mm that had cracking both in the weld zone and in the plate material due to the severity of the close proximity blast.

In the five partial-penetration coupons with cracking solely in the weld zone, the crack location configuration varied from coupon to coupon and along the length of the cracks in individual coupons. The most common crack location configuration, however, was adjacent to the fusion boundary between the BisPlate HHA and the weld on the tension side and through the weld metal on the compression side. Figure 19 is a polished and etched section taken through the fracture surface of coupon 75-12 showing this predominant crack location configuration.

Figure 20 shows the range of crack location configurations that were observed in the cracked partial penetration coupons. Crack configurations often varied along the length of the crack.

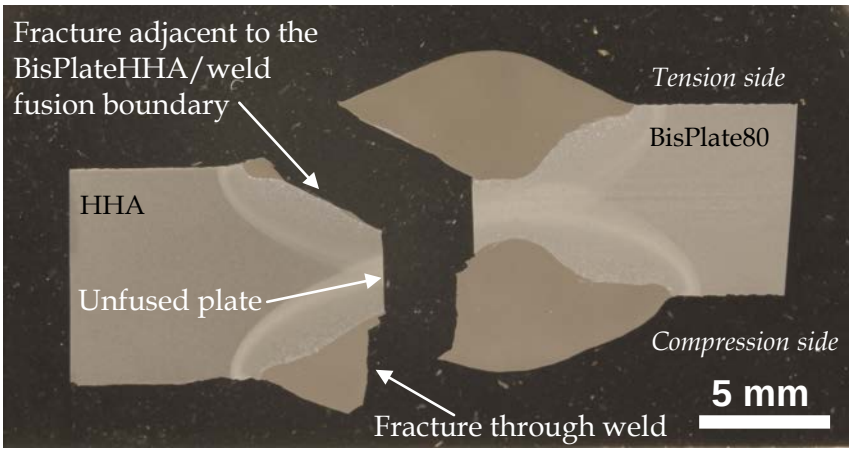

Figure 19: A polished and etched section of a failed partial-penetration coupon (75-12) illustrating the most common crack location configuration.

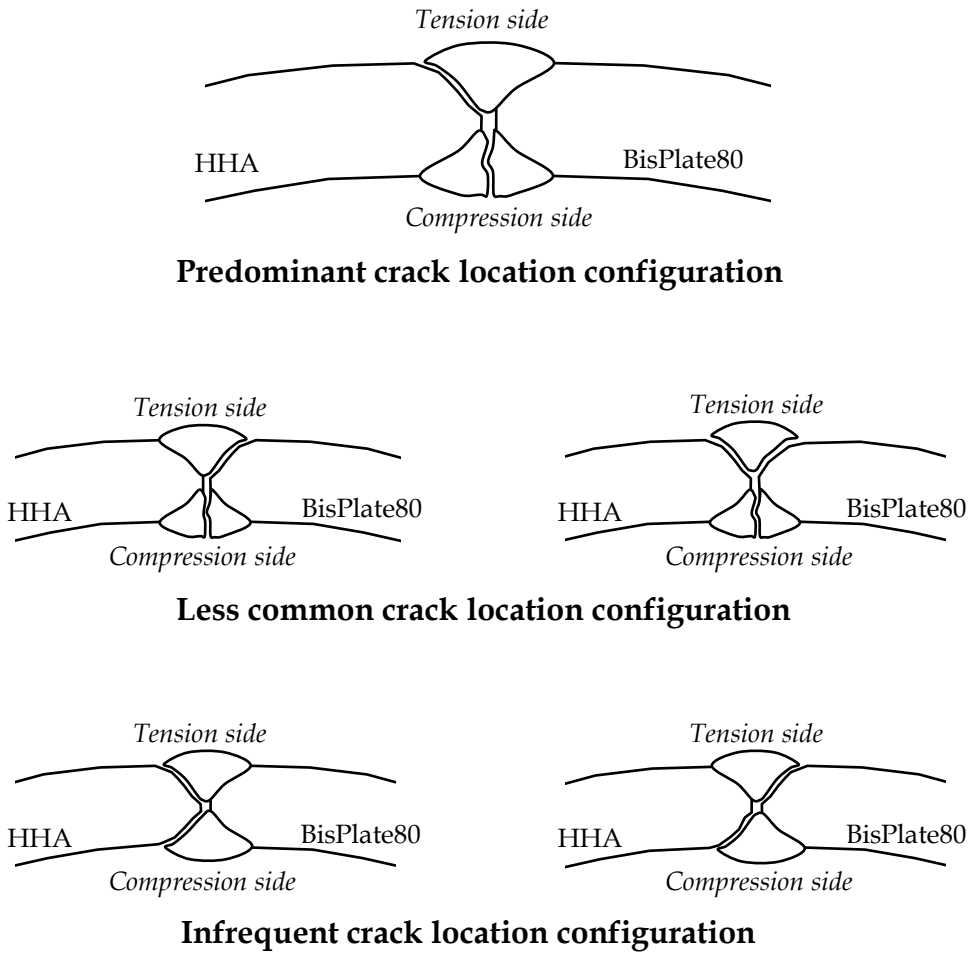

Figure 20: Crack location configurations observed in cracked partial-penetration coupons. Crack configurations often varied along the length of the crack.

5.2.2 Crack Location in Full-penetration Coupons

Three full-penetration coupons exhibited cracking. These are shown in Figure 21, Figure 22 and Figure 23, corresponding to coupons 100-05, 100-03 and 100-10, respectively. Of these coupons, the test with the largest stand-off distance, 154 mm (Figure 21, coupon 100-05), exhibited cracking only in the BisPlate80 parent metal, 20 mm from the weld toe on the tension side through to 8 mm from the weld toe on the compression side. The crack was located outside the HAZ, and only grew to approximately 30 mm in length. The fracture path was at a 45° angle to the plate surface which is characteristic of a slant fracture resulting from tensile tearing. A sketch of the cross-section 'A-A' through this crack is shown in Figure 21 (b).

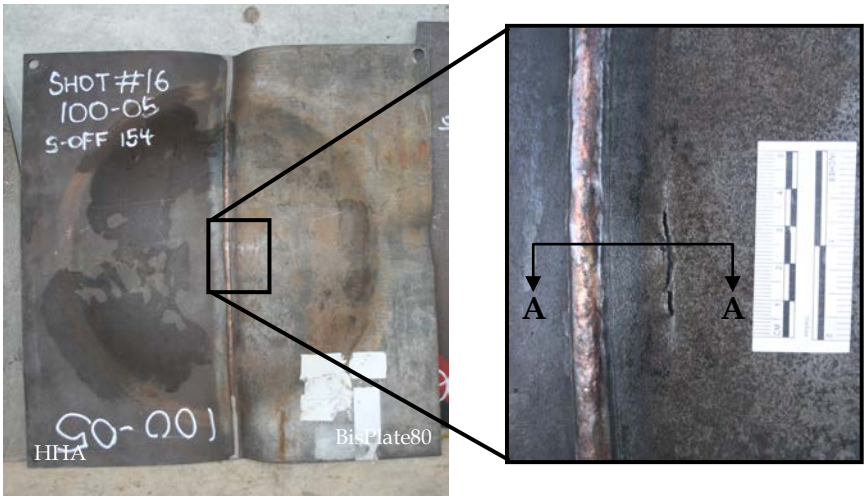

(a)

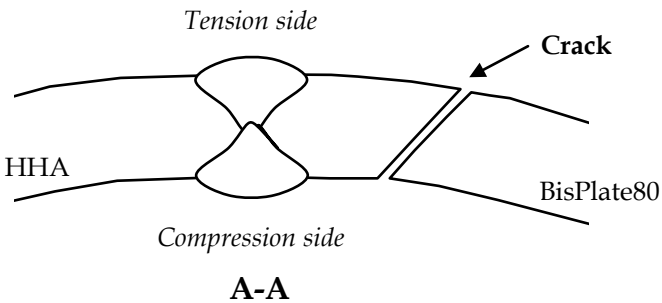

(b)

Figure 21: Full-penetration coupon (coupon 100-05) tested at a stand-off distance of 154 mm, (a) photograph and close-up and (b) schematic of cross-section 'A-A'.

The coupon tested at a stand-off distance of 150 mm, coupon 100-03 shown in Figure 22, showed similar cracking to coupon 100-05, i.e. cracking in the BisPlate80 parent metal near to the apex of the deformation. A sketch of the cross-section of this cracking is shown in Figure 22 (b). Further from the apex, there was additional extensive cracking adjacent to

the weld. The fracture path of this additional cracking extended from the weld toe, in the BisPlate80 on the tension side, through the BisPlate80 at approximately a 45° angle away from the weld, meeting the BisPlate80 plate surface on the compression side, approximately 8 mm from the weld toe. A schematic of this cracking has been included in Figure 22 (c).

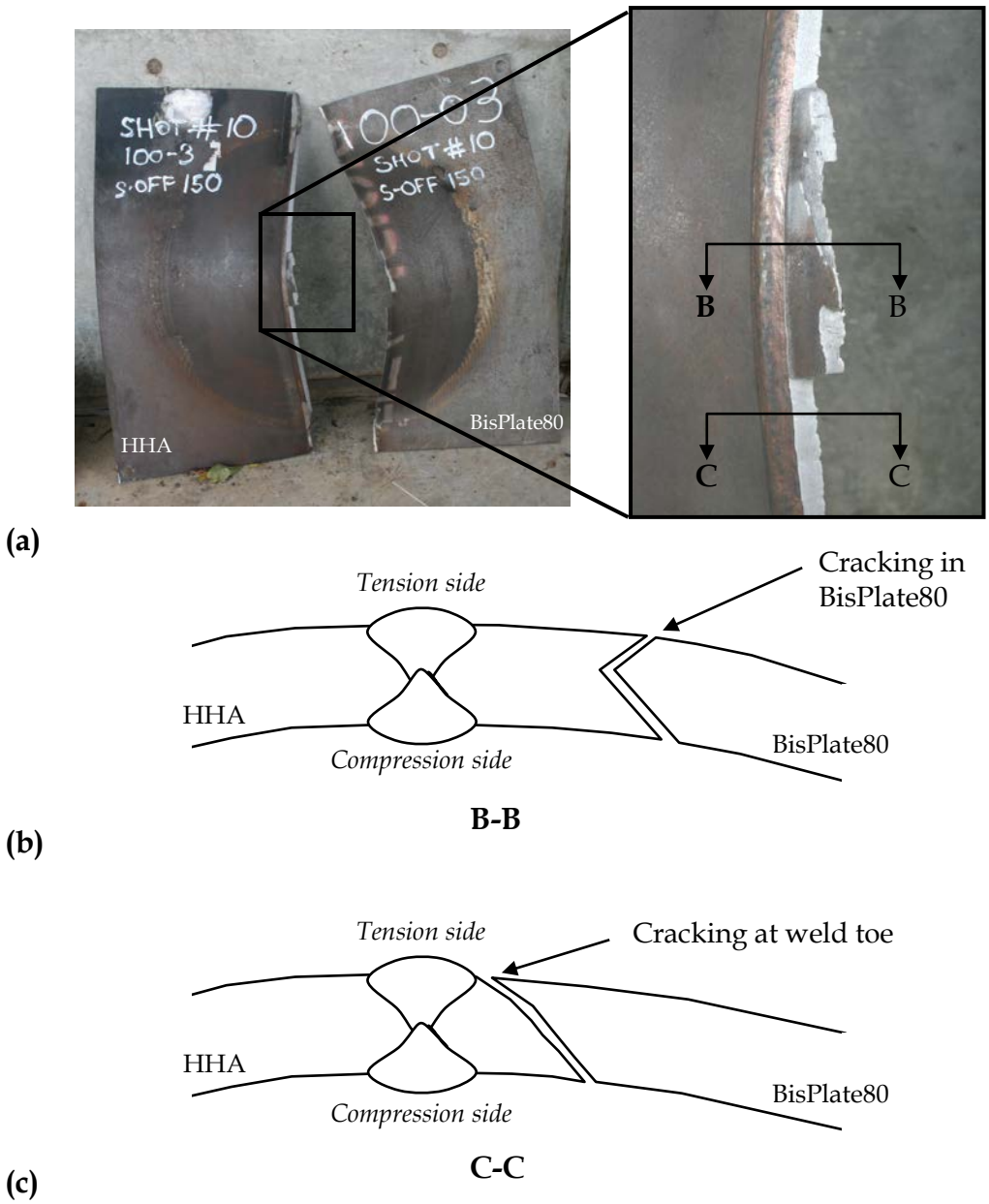

Figure 22: Full-penetration coupon (coupon 100-03) tested at a stand-off distance of 150 mm, (a) a photograph and close-up, (b) a schematic of cross-section 'B-B' and (c) a schematic of cross-section 'C-C'.

The full-penetration coupon tested at a 117 mm stand-off, coupon 100-10, was significantly deformed by the blast and the BisPlate80 and weld toe cracking described above was accompanied by significant cracking into both the BisPlate80 and the BisPlate HHA as

shown in Figure 23. The centre of the coupon tested at a stand-off of 117 mm was so grossly deformed that it came into contact with the floor of the blast chamber.

Figure 23: The full-penetration coupon (coupon 100-10) tested at a stand-off distance of 117 mm exhibited cracking in the weld zone and in both plate materials.

5.2.3 Crack Location in Nominally Full-penetration Coupons with Incomplete Penetration

The two nominally full-penetration coupons (100-02 and 100-04) containing lengths of incomplete penetration (i.e. 90% penetration) were tested at the greatest stand-off at which cracking was observed in the full-penetration coupons — 154 mm. Cracking was observed in only one of these coupons, Coupon 100-04 shown in Figure 24, which cracked in the BisPlate80 parent metal in a manner similar to the full-penetration coupon tested at the same stand-off, Figure 21.

Figure 24: BisPlate80 cracking observed in coupon 100-04 which contains incomplete penetration (90% penetration) and was tested at a stand-off of 154 mm.

Sections were taken through both of these nominally full-penetration coupons to investigate the possibility of crack growth originating at the incomplete penetration

discontinuity. The incomplete penetration defect in coupon 100-04, shown in Figure 25 (a), does not show evidence of crack growth resulting from the blast.

The incomplete penetration defect in coupon 100-02, shown in Figure 25 (b), demonstrates some evidence of cracking at the end of the incomplete penetration defect. However, it is not clear whether this defect has extended as a result of the blast or whether it is a solidification crack which occurred at the time of welding. In either case the crack is inconsequential in the context of the current study.

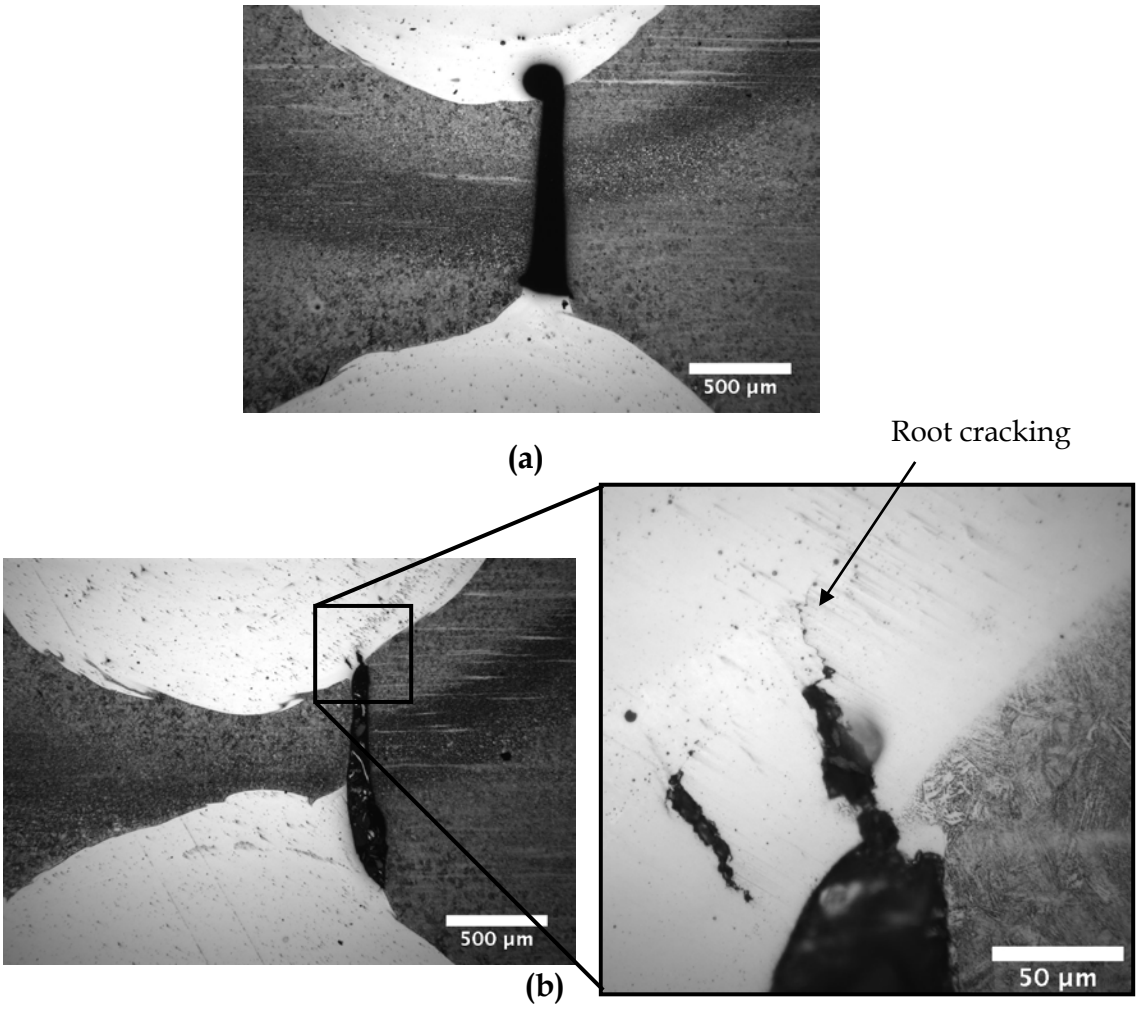

Figure 25: Micrographs of the incomplete penetration (~90% penetration) defects in (a) coupon 100-04 and (b) coupon 100-02.

5.3 Fracture Characteristics

5.3.1 Partial-penetration Coupon

The fracture characteristics of the tension side cracking through the plate material and the weld metal of coupon 75-12 are shown in Figure 26 and Figure 27, respectively. Both images show evidence of ductile fracture and were representative of the majority of the

fracture surfaces. The coupon 75-12 fracture path diagram, shown in Figure 28, indicates the locations where these images were taken.

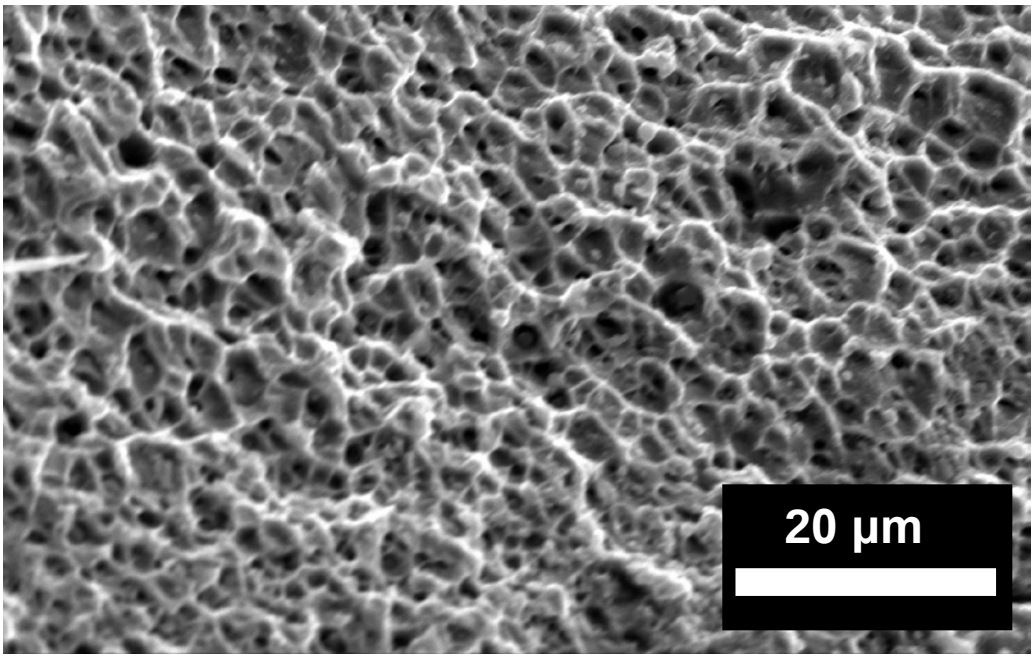

Figure 26: Scanning electron microscope images of ductility on the fracture surface of the tension side crack which propagated through the weld metal (coupon 75-12).

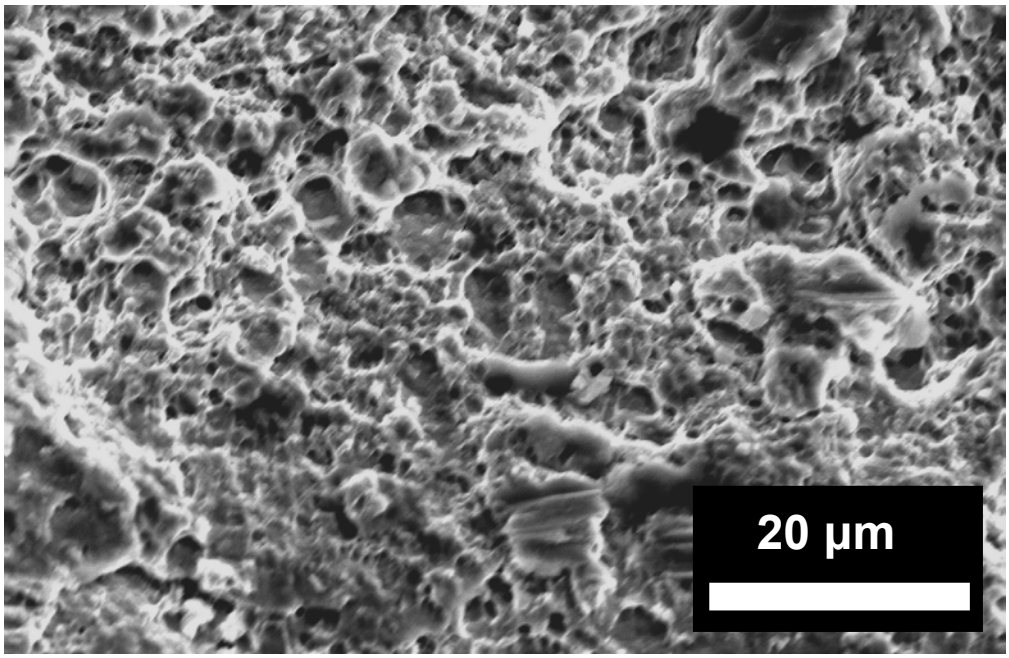

Figure 27: Ductile features on the fracture surface of the tension side crack which propagated through the BisPlate80 material of coupon 75-12. Some smearing damage has occurred after crack formation.

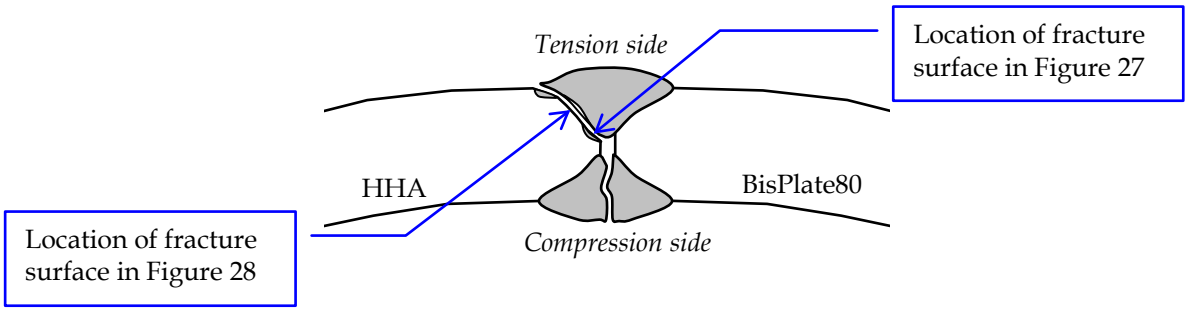

Figure 28: Diagram of the fracture path of coupon 75-12 showing the location where fracture surface imagery was taken using the scanning electron microscope.

5.3.2 Full-penetration Coupon

Cracking in the full-penetration coupons was observed to initiate in the BisPlate80 approximately 20 mm from weld toe (this is outside the HAZ). These cracks were at a 45° angle to the plate surface and necking was observed near the fracture. Figure 29 is a scanning electron microscope image taken of the fracture surface of the crack in coupon 100-04 illustrating the ductile nature of the fracture.

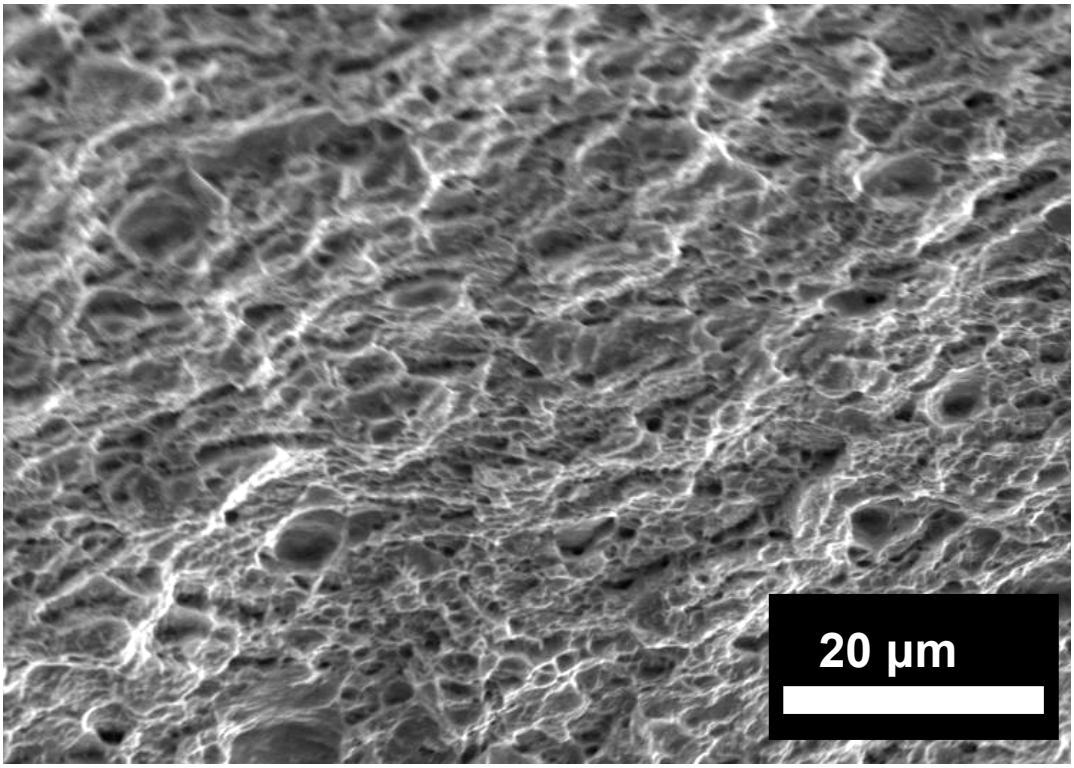

Figure 29: Ductile features on the fracture surface of the crack in the BisPlate80 plate of coupon 100-04.

6. Discussion

The aim of this study was to determine whether incomplete weld penetration degrades the blast resistance of plates of BisPlate80 welded to BisPlate HHA.

The welds in the partial-penetration and the full-penetrations coupons were found to be comparable with respect to material hardness (both weld and plate) and extent of the heat affected zone. Similarly, the dilution and composition results determined using semi-quantitative methods showed no obvious disparity between the full-penetration weld and the partial-penetration weld. The weld reinforcement area for the partial-penetration welds was less than that of the full-penetration welds. This is a result of the welding parameters that were selected to generate the specified amount of penetration.

The explosive loading produced by the 143 mm diameter 2.1 kg spherical charge is estimated to have a fireball radius of over 2 meters [12]. The largest stand-off distance was 515 mm and the loading on the plates is predominantly due to the dynamic pressure of the impingement of the expanding detonation products. This is simplified compared to the loading experienced by armoured vehicles where loading can be a combination of many variables such as: the explosive used, shockwave, detonation products, soil ejecta and fragmentation. The blast loading for this current experiment was not intended to directly replicate loading likely to be experienced in theatre. Rather, it was selected to provide a known, quantifiable and repeatable blast loading to apply to the test coupons. A simplified test set-up, when compared to full-scale vehicle tests, has the advantage of enhanced repeatability, lower cost, faster test turnaround and a reduced number of variables to control. Figure 30 is an illustration of the simplifications made in order to control variables. In this test the degree of penetration and the stand-off distance (severity of loading) were the only significant variables.

The simplified loading (varying stand-off distance only) used in this test successfully generated a spectrum of coupon responses ranging from virtually unaffected through to catastrophic deformation and cracking.

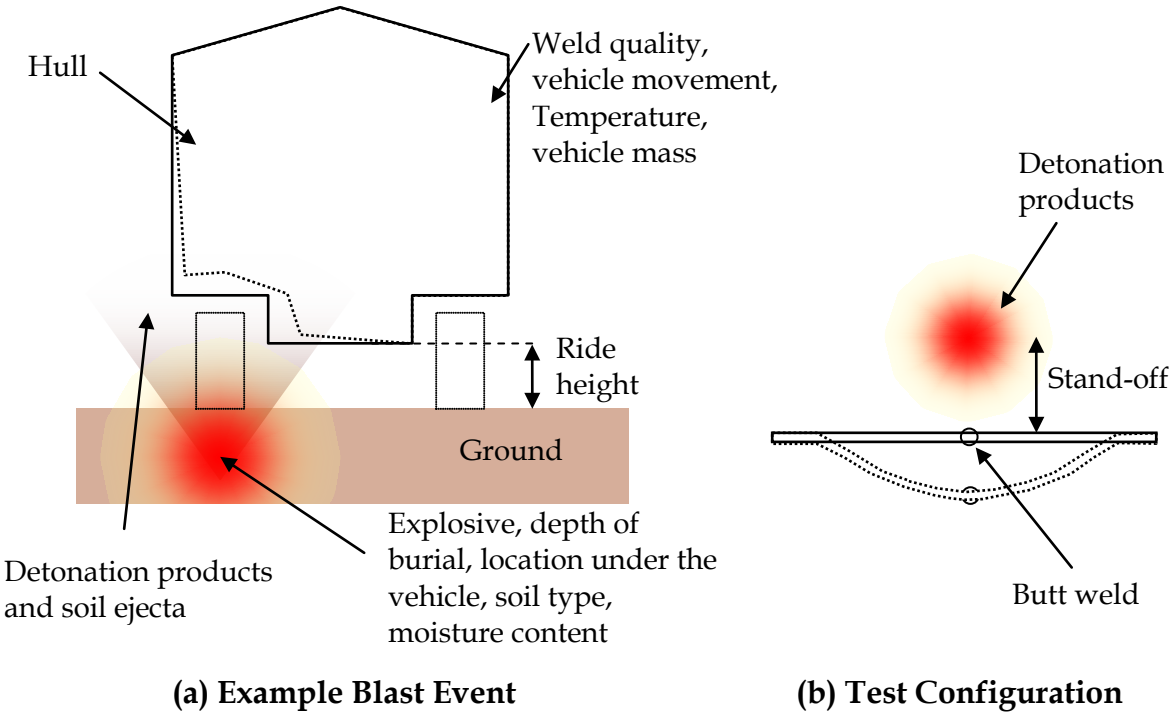

Figure 30: Illustration of the many variables and differences between loading on (a) a vehicle in a full scale test and (b) the simplified test configuration used in this experiment.

The deformation in the tested coupons increased steadily with decreasing stand-off as shown in Figure 14, consistent with larger blast loads producing more deformation. An apparent outlier to this trend was the coupon tested at a stand-off distance of 165 mm which was measured to have more deformation than the coupon tested at 158 mm. This apparent inconsistency is likely to be an artefact of the measurement technique as the deformation resulting from these small stand-off tests displayed, not only bulging at the centre, but also warping and buckling at the edges of the plate. As the plate edges were used as a baseline for the deformation measurement they will have contributed some error. In contrast, the thinning measurements for the same coupons, shown in Figure 15, show greater thinning in the coupon tested at 158 mm than the coupon tested at 165 mm, as expected.

The full-penetration welds withstood, without coupon cracking, closer blasts, and correspondingly greater loading, than their partial-penetration weld counterparts. Evidence for this is the difference between the threshold stand-off distances for failure of the two weld conditions shown in Figure 17. In addition, the full-penetration welded coupons were found to accommodate approximately 50% more deformation before experiencing cracking, as observed in Figure 13. This result is (i) partly due to there being 35% less load bearing cross-section in the partial-penetration weld as compared to the full-penetration weld and (ii) partly due to the presence of the crack-like flaw resulting from the partial penetration weld.

The reduced load bearing cross-section in the partial-penetration welds occurs because the unfused plate has no load carrying capacity and because of the slightly larger weld

reinforcement in the full-penetration welds. However, despite the smaller load bearing cross-section of the partial-penetration weld, the deformation and thinning behaviour for these coupons where cracking did not occur (see Figure 14 and Figure 15) was consistent with that of the full-penetration coupons that did not experience cracking.

The crack-like flaw found in the root of the partial penetration welds acts as a stress concentrator and is a favourable site for crack growth. This accounts for the differing location of cracking in the partial and full-penetration welded coupons. The partial-penetration coupons exhibited cracking in the weld zone which always included the unfused area of plate i.e. the crack-like flaw.

In contrast to the partial-penetration weld, the greater load bearing cross-section of the full-penetration weld reduced the stress levels in the weld metal, thus avoiding strain localisation and associated tensile tearing in the weld zone. This allowed the coupon to continue deforming (albeit asymmetrically due to the different plate material properties) without weld zone cracking. Given sufficient loading, cracking in the full-penetration coupons initiated 15 to 20 mm from the weld toe in the BisPlate80 plate material. This was the apex of the bulge, the area of greatest deformation[3], and was located outside the weld zone (weld material and HAZ). When the loading only just exceeded the full-penetration coupon failure threshold, as defined in section 3.1, the BisPlate80 crack propagation was arrested within the plate, as is seen in the response of coupon 100-05.

As the loading is increased beyond this failure threshold, the stress in the plate will be transferred, following the initial cracking in the BisPlate80, to the weld zone material on either side of the initial crack (refer to coupon 100-03 shown in Figure 22). Despite the deformation being less in this location, the additional cracking is located here due to the stress concentration located at the BisPlate80 weld toe on the tension side of the plate.

The ability of full-penetration welds to accommodate deformation and their greater resistance to cracking under blast loading has the potential to increase the survivability of structures subjected to blast loading. Conversely, the presence of continuous incomplete penetration defects is likely to decrease the blast performance of welded structures.

However, it is likely that there will be some threshold amount of incomplete penetration below which the blast performance will not be adversely affected. For example, the performance of the two nominally full-penetration weld coupons that contained approximately 90% penetration (coupon 100-04 and 100-02) behaved in a manner that was consistent with the full-penetration coupons, despite the presence of the incomplete penetration defects.

All the full-penetration weld coupons had some minor discontinuities present, however, the weld remained intact and cracking occurred in the BisPlate80 plate material. This indicates that minor discontinuities did not adversely affect the performance of the welded joints and suggests that there may be some critical discontinuity length and size for which

[3] The asymmetric nature of the bulge observed in Figure 13 results from the large difference in the strength of the BisPlate80 and the BisPlate HHA.

the blast performance of the weld is not adversely affected. Knowledge of a critical discontinuity length could be used to inform weld quality specifications.

7. Conclusions

1. The test methodology was demonstrated to be a low cost, rapid and versatile approach to demonstrate the relative blast resistance of full-penetration welds as compared to those with partial-penetration. The sub-system test successfully allowed for this aspect of welded armoured vehicle performance to be examined and could be adopted to investigate other weld characteristics, for example, weld geometry. The response of the coupons to the blast varied from very little deformation, experienced at the greatest stand-off used in the test series, to total plate destruction at the closest stand-off. Between these extremes the deformation, thinning and cracking results exhibited consistent trends as a function of the test stand-off distance.

2. Incomplete weld penetration significantly degrades the blast resistance of plates of BisPlate80 steel welded to BisPlate High Hardness Armour (BisPlate HHA) steel.

3. It has been demonstrated that full-penetration welds will withstand, without cracking, closer blasts, and correspondingly greater blast loading, than partial-penetration welds.

4. The full-penetration coupons in this experiment withstood 50% more deformation before cracking than the partial-penetration coupons.

8. Future Analysis

As noted in the discussion the experimental joint geometry was a simple butt weld while vehicle joint geometry can be more complex. Future experiments could be conducted that more faithfully represent the joint geometry of the vehicle and could include investigations into determining the plate edge configuration/weld joint detail with the greatest blast resistance for future vehicle designs.

For the tested coupons, the incomplete penetration extended the full length of the coupon. This work indicates that there may be some critical length and size dimensions of partial-penetration for which the blast performance of the weld is not adversely affected. The effect of the size (length and percentage penetration) of the welding discontinuity could be investigated to further inform manufacturing specifications.

Acknowledgements

(U) This work would not have been possible without the assistance from many people within and external to DSTO. From the University of Wollongong, Lenka Kuzmikova prepared and performed the robotic welding, while John Norrish provided advice and logistical support. At DSTO Edinburgh, John Williams performed the duties of firing and safety officer. Trevor Delaney provided logistical support and helpful advice for conducting an efficient trial. Kate Ackland assisted for the duration of the trial and her excellent suggestions were appreciated. Zoran Sterjovski provided advice on welding and degaussing. Choi Chang-ho provided instruction regarding temperature data acquisition.

Joe Donato has provided continued helpful advice and assistance throughout the work from inception to documentation in relation the EBT test procedure, welding, instrumentation, radiography, trial preparation, documentation and approvals.

References

1. P. P. Puzak and W. S. Pellini (1961) *Standard Evaluation Procedure for Explosion Bulge Testing (Weldments)*. NRL Memorandum Report 1255, Washington D.C., U.S. Naval Research Laboratory
2. *Standard Procedures for Explosion Testing Ferrous and Non-Ferrous Metallic Materials and Weldments*. (1990) MIL-STD-2149A (SH), [Test Method Standard] Department of Defence
3. J. R. Matthews, C. V. Hyatt and J. F. Porter (2001) Future Treatment of Weld Acceptance: The Significance of Incomplete Fusion Discontinuities in Low Structural Transition Temperature Gas Metal Arc Weldments. *Materials Evaluation* (April 2001) 523-530
4. L. N. Pussegoda and L. Malik (1996) *Metallurgical evaluation of defects in explosively loaded plates*. DREA CR/95/501, Kanata, Ontario, Canada, Defence Research Establishment Atlantic
5. *Base materials for critical application: requirements for low alloy steel plate, forgings, castings, shapes, bars, and heads of HY-80/100/130 and HSLA-80/0100*. (2002) T9074-BD-GIB-010/0300, [NAVSEA Technical Publication,] United States Navy Sea Systems Command (NAVSEA)
6. Z. Sterjovski, J. Donato and J. L. Davidson (2009) *Explosive Load Testing of the Grade DH36 and DH55 Steel Plates Selected for the Air Warfare Destroyer*. DSTO-CR-2507-2009, [Client Report] Melbourne, Defence Science and Technology Organisation
7. *Temperature Mapping in DH36 and DH55 Steel Plate Subject to Explosion Bulge Testing*. (2012) [Personal Communication: Data Sheet] Received by E. L. Frain from: J. Donato, Melbourne, Defence Science and Technology Organisation 16 July 2012
8. J. L. Davidson (1995) Hydrogen-Induced Cracking Of Low Carbon - Low Alloy Steel Weldments In: G. Schaffer (ed.) *Materials Forum*. Vol. 19, Fracture and Failure. North Melbourne, The Institute of Engineers, Australia
9. J. Wilson (1978) The development of welding techniques for British fighting vehicles. In: *International Conference on Trends in Steel and Consumables for Welding*, London: 13-16 November 1978
10. J. C. Ritter, B. F. Dixon and N. J. Baldwin (1989) Deformation and weld repair of armour steel. *Materials Forum* **13** 216-224
11. *Radiographic Reference Standards and Radiographic Procedures for Partial-Penetration Steel Welds*. (1998) MIL-STD-1894B, [Standard Practice] U. S. Department of Defence
12. J. B. Gayle and J. W. Bransford (1965) *Size and duration of fireballs from propellant explosives*. TM X-53314, National Aeronautics and Space Administration

Appendix A: Manufacturer's Material Data Sheets

Plate Material Specifications

August 2004

Bisalloy Steels
Bisalloy Steels Pty Ltd
PO Box 1256,
Unanderra, NSW, Australia, 2526
Ph - +61 2 4272 0444 Fax - +61 2 4272 0456
Email – bismail@bisalloy.com.au
Web - http://www.bisalloy.com.au/

BISPLATE 80

Applications	BISPLATE 80 – a low alloy, high strength steel plate with a yield strength three times that of carbon steel and featuring low carbon, excellent notch toughness and good weldability and formability. Utilising the high strength properties of BISPLATE 80 allows reduction in section thickness without loss of structural integrity. The following are some applications where the strength advantage has been realised: ▪ Transport Equipment (low loaders) ▪ High Rise Buildings (columns) ▪ Bridges ▪ Excavator Buckets ▪ Storage Tanks ▪ Lifting Equipment (mobile cranes/container handling equipment) ▪ Mining Equipment (dump truck trays / longwall roof supports) ▪ Induced Draft Fans

Chemical Composition

Thickness		C	P	Mn	Si	S	Cr	Mo	B	CE (IIW)	PCM
5–<16	Typical	0.16	0.010	1.10	0.20	0.003	-	0.20	0.0010	0.40	0.25
≥16-80	Typical	0.18	0.010	1.40	0.20	0.003	0.20	0.20	0.0010	0.50	0.29
>80-100	Typical	0.16	0.010	1.15	0.20	0.003	0.90	0.20	0.0010	0.58	0.30

Mechanical Properties

	0.2% Proof Stress	Tensile Strength	Elongation in 50 mm GL
Specification	690 MPa (min)*	790 – 930 MPa*	18% (min)*
Typical	750 MPa	830 MPa	26%

Charpy Impact Properties

	Longitudinal, -20°C (10mm x 10mm)
Specification	40 J (min)*
Typical	160 J

Hardness	Typical 255 HB
Testing	BISPLATE 80 is manufactured in accordance with AS/NZS 3597 Grade 700. All testing is NATA approved.
Reference Specifications	Welding according to AS/NZS 1554 parts 4 and 5, WTIA Technical Note 15
Equivalent Specifications	BISPLATE 80 is equivalent to • ASTM A514 • ISO 4950-3 Grade E690 • ISO 9328-4 Grade P690TQ • EN 10137-2 Grade S690Q • JIS G3128
Manufacturing Tolerances	In accordance with AS/NZS 1365. Tighter tolerances may be available on negotiation.
Surface Finish	Shotblasted
Plate Colour Code	Pink
Fabrication	For advice on fabrication refer to relevant Bisalloy technical brochures. Contact Bisalloy direct or visit www.bisalloy.com.au.

* Dependent on plate thickness

BISPLATE HHA

High Hardness Armour Plate

Bisalloy Steels

Bisalloy Steels Pty Ltd
PO Box 1246, Unanderra, NSW, Australia, 2526
Ph: +61 2 4272 0444 / Fax: +61 2 4272 0456
Email: bismail@bisalloy.com.au
Web: http://www.bisalloy.com.au

Applications

BISPLATE High Hardness Armour (BISPLATE HHA) - a quenched and tempered steel armour plate suitable for use in both military and civil applications where light weight and resistance to ballistic projectiles is required.

Chemical Composition (% weight)

The chemical specification conforms to the requirements of MIL-A-46100, although tighter so as to optimise the material's performance. Chemical analyses are taken on a per heat basis.

Thickness		C	P	Mn	Si	S	Ni	Cr	Mo	B	CE(IIW)	PCM
5-25[1]	Maximum	0.32	0.025	0.80	0.50	0.005	0.50	1.20	0.30	0.002	0.61*	0.40*

Mechanical Properties (AS 1391)

	0.2% Proof Stress	Tensile Strength	Elongation in 50mm GL
Typical	1400 MPa	1640 MPa	14%

Charpy Impact Properties (AS 1544.2)

Thickness	Test Piece	Min Energy, Transverse, -40°C	Min Energy, Longitudinal, -40°C
5mm	10 x thk	by agreement	by agreement
6-<9.5mm	10 x 5	8J	10J
9.5-<12mm	10 x 7.5	12J	15J
≥12mm	10 x 10	16J	20J

Hardness (AS 1816)

Specification	477 - 534 HB
Typical	500 HB

Thickness Tolerance

Thickness	Special Tolerance
5-25mm	-0.0 + 1.0

Test Frequency

Per Plate	Hardness.
Per Batch	Charpy (L), Charpy (T).
By Agreement	Thickness, Tensile, Ballistic Properties, Product Analysis.

Ballistic Properties

AS 2343 Part 2 - Bullet Resistant Panels for Interior: Opaque Panels

Class[2]	Calibre	Ammunition	Velocity @ Distance From Muzzle	Range	Min Thickness
G2	44 Magnum	15.6g lead semi-wad cutter bullet	488 ± 10m/s @ 1.5m	3m	6mm[3]
S0	12 Gauge (Full Choke)	12 gauge 70mm high velocity magnum 32g SG shot	403 ± 10m/s @ 1.5m	3m	6mm[3]
S1	12 Gauge (Full Choke)	12 gauge 70mm 24.8g single slug	477 ± 10m/s @ 1.5m	3m	6mm[3]
R1	5.56mm	M193 5.56mm 3.6g full metal case bullet	980 ± 15m/s @ 5m	10m	10mm[3]
R2	7.62mm	NATO standard 7.62mm 9.3g full metal case bullet	853 ± 10m/s @ 5m	10m	6mm

Equivalent Specification

BISPLATE HHA conforms to the requirements of MIL - A - 46100.

Surface Finish

Shotblasted.

Fabrication

For advice on fabrication refer to relevant Bisalloy technical brochures. Contact Bisalloy direct or visit www.bisalloy.com.au

* Typical. [1] Other thicknesses may be available on application. [2] Class G - Hand Gun, Class S - Shotgun, Class R - Rifles.
[3] Standard thickness produced. Minimum thickness required is less than stated thickness. Please contact Bisalloy for further information.

PLEASE NOTE: Every care has been taken to ensure the accuracy of the information contained in this manual which supersedes earlier publications, however Bisalloy Steels shall not be liable for any loss or damage whatsoever caused from the application of such information. Typical values are provided for reference information only and no guarantee is given that a specific plate will provide these properties. Information is subject to change without notice.

December 2004

Consumable Material Specifications

TETRA S 20 9 3-G

CLASSIFICATION

ASME IIC SFA 5.22 / AWS A 5.22:	(E308MoT0-4 - E308MoT0-1) nearest
EN ISO 17633-A:	T 20 10 3 R M 3 - T 20 10 3 R C 3
EN ISO 17633-B:	TS308Mo-FB0*
*Mo may exceed 3.0 %, Si may exceed 0.65 % and Cr may exceed 21.0 %	
ASME IX Qualification	QW432 F-N° 6 QW442 A-N° 8

DESCRIPTION

- Rutile flux cored stainless steel wire for gas shielded metal arc welding
- 20% chromium - 9% nickel - 3% molybdenum deposit
- Exceptional resistance to moisture pick up
- Attractive bead appearance, automatic slag release, very good penetration and high productivity
- Excellent X-ray soundness
- Maximum performances in the horizontal and downhand positions
- Welded with classical economical Ar-CO_2 mixtures or CO_2

APPLICATIONS

Tetra S 20 9 3-G offers a strong, tough crack free deposit suitable for tank and other military vehicle fabrication. It is also useful for welding high tensile steels, for joining 13% manganese steels, hardenable steels or wear-resistant steels.

It is as a multi-purpose wire for maintenance and for welding dissimilar joints.

TYPICAL ALL-WELD METAL ANALYSIS

C	Mn	Si	Cr	Ni	Mo	S	P
0.05	1.50	0.80	20.5	9.70	2.90	0.008	0.020

Typical ferrite level: 25%

MINIMUM ALL-WELD METAL MECHANICAL PROPERTIES

Rm [MPa]	Rp0.2% [MPa]	A_5 [%]	KV [J]
620	150	20	-20°C : 32

TYPICAL ALL-WELD METAL MECHANICAL PROPERTIES

Rm [MPa]	Rp0.2%[MPa]	A_5 [%]	KV [J]
710	530	30	-20°C : 45

SHIELDING GAS

M20 (Ar + 5 - ≤ 15% CO_2), M21 (Ar + 15 - 25% CO_2) gas mixtures, or C1 (CO_2) according to EN ISO 14175

OPERATING CONDITIONS

Diameter [mm]	Current type	Intensity [A]	Voltage [V]	Stick-out [mm]	Gas flow
1.2	DC (+)	100 - 280	23 - 33	10 - 25	12 - 20 l/min.
1.6	DC (+)	150 - 400	23 - 35	10 - 25	12 - 20 l/min.

WELDING POSITIONS

EN ISO 6947:	PA, PB.
ASME IX:	1G, 1F, 2F.

PACKAGING

Diameter	1.2 mm		1.6 mm
	EN ISO 544 – ASME II C SFA-5.2 M		
Spool type	S200	BS300	BS300
Weight	5 kg	15 kg	15 kg

Other packaging: please consult us

http://www.welding-alloys.com/products-services/wa-welding-consumables/joining-cored-wires/welding-of-highly-alloyed-steels/tetra-s-20-9-3-g.html

Appendix B: Quantitative Chemical Analysis

The quantitative chemical analysis was conducted by Spectrometer Services Pty. Ltd. using inductively coupled plasma atomic emission spectroscopy.

	BisPlate HHA (coupon sample)		**BisPlate80 (coupon sample)**	
	Analysis Results (%wt)	Material Specifications Max (%wt)	Analysis Results (%wt)	Material Specifications Typical (%wt)
C	0.28 ± 0.05	0.32	0.15 ± 0.04	0.16
Mn	0.30 ± 0.05	0.80	1.19 ± 0.03	1.10
Si	0.28 ± 0.05	0.50	0.24 ± 0.05	0.20
S	0.01 ± 0.002	0.005	0.01 ± 0.002	0.003
P	0.01 ± 0.002	0.025	0.02 ± 0.002	0.010
Ni	0.19 ± 0.04	0.50	0.06 ± 0.02	-
Cr	0.99 ± 0.03	1.20	0.12 ± 0.03	-
Mo	0.27 ± 0.05	0.30	0.24 ± 0.05	0.20
Cu	<0.01	-	0.02 ± 0.004	-
V	0.03 ± 0.006	-	0.01 ± 0.002	-
Nb	<0.01	-	<0.01	-
Ti	0.02 ± 0.004	-	0.02 ± 0.002	-
Al	0.024 ± 0.005	-	0.053 ± 0.005	-
B	0.0009 ±0.0002	0.002	0.0008 ± 0.0002	0.0010

Appendix C: Semi-Quantitative Compositional Analysis of a Partial-penetration and Full-penetration coupon

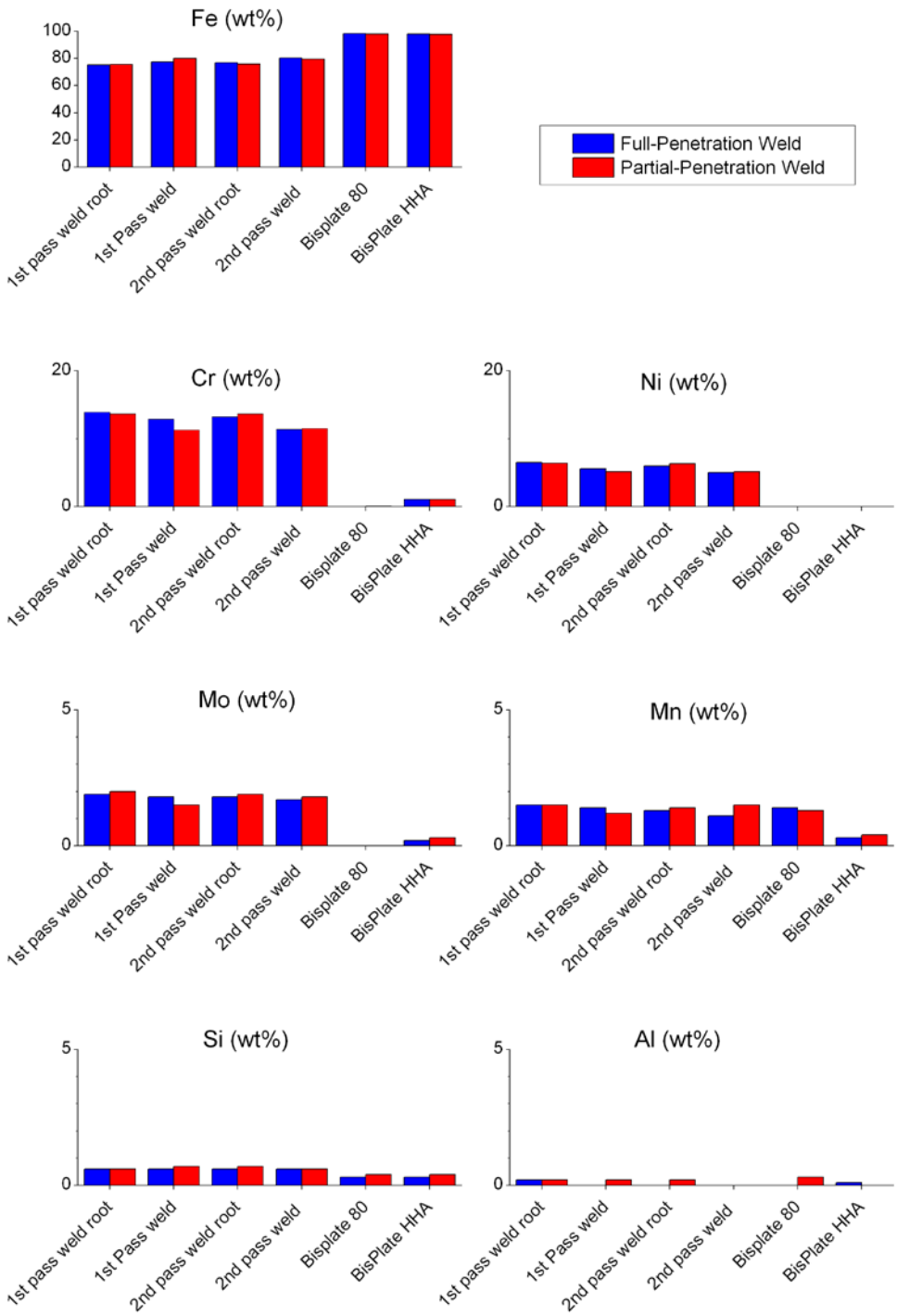

Appendix D: Coupon Deformation

Plate ID	75-02	75-05	75-11	75-12	75-06	75-13	75-14	75-01	75-04	75-03
Stand-off	117 mm	182 mm	200 mm	208 mm	208 mm	212 mm	216 mm	253 mm	312 mm	515 mm

Plate ID	100-10	100-03	100-05	100-04	100-02	100-06	100-08	100-01
Stand-off	117 mm	150 mm	154 mm	154 mm	154 mm	158 mm	165 mm	182 mm

Specified full-penetration weld coupons containing partial-penetration defects (90%)

Appendix E: Thinning of Coupons with Cracking

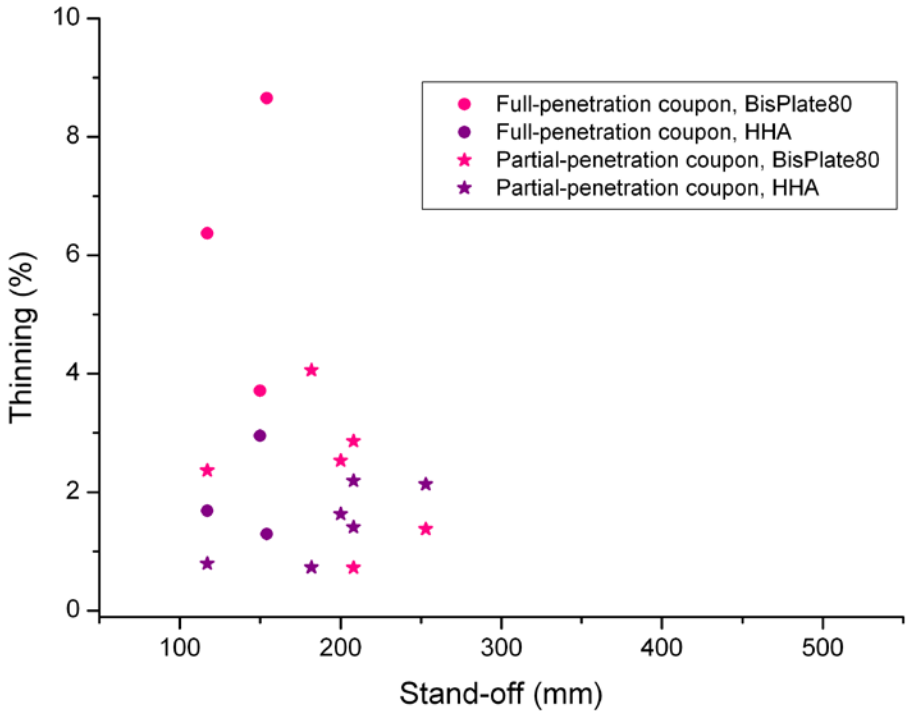

DEFENCE SCIENCE AND TECHNOLOGY ORGANISATION
DOCUMENT CONTROL DATA

1. DLM/CAVEAT (OF DOCUMENT)

2. TITLE

The Effect of Weld Penetration on Blast Performance of Welded Panels

3. SECURITY CLASSIFICATION (FOR UNCLASSIFIED REPORTS THAT ARE LIMITED RELEASE USE (L) NEXT TO DOCUMENT CLASSIFICATION)

Document	(U)
Title	(U)
Abstract	(U)

4. AUTHOR(S)

Emily Frain and Len Davidson

5. CORPORATE AUTHOR

DSTO Defence Science and Technology Organisation
506 Lorimer St
Fishermans Bend Victoria 3207 Australia

6a. DSTO NUMBER	6b. AR NUMBER	6c. TYPE OF REPORT	7. DOCUMENT DATE
DSTO-TR-3017	AR-016-068	Technical Report	August 2014

8. FILE NUMBER	9. TASK NUMBER	10. TASK SPONSOR	11. NO. OF PAGES	12. NO. OF REFERENCES
2013/1141157/1	CDF 07/331	COMD ADF CIED TF (through: SOSc to CIEDTF)	42	12

13. DOWNGRADING/DELIMITING INSTRUCTIONS

To be reviewed three years after date of publication

14. RELEASE AUTHORITY

Chief, Maritime Division

15. SECONDARY RELEASE STATEMENT OF THIS DOCUMENT

Approved for Public Release

OVERSEAS ENQUIRIES OUTSIDE STATED LIMITATIONS SHOULD BE REFERRED THROUGH DOCUMENT EXCHANGE, PO BOX 1500, EDINBURGH, SA 5111

16. DELIBERATE ANNOUNCEMENT

No Limitations

17. CITATION IN OTHER DOCUMENTS Yes

18. DSTO RESEARCH LIBRARY THESAURUS

Weld Quality, Blast

19. ABSTRACT

A modified explosion bulge test method was used demonstrate the difference in performance of full-penetration (nominally 100%) welds and partial-penetration (nominally 70%) welds under blast loading. The welded coupons consisted of armour steel plate, Bisalloy BisPlate High Hardness Armour steel, welded to Bisalloy BisPlate80 steel with an austenitic filler material, TETRA S 20 9 3-G . If was found that full-penetration welds will withstand, without cracking, closer blasts, and correspondingly greater blast loading, than partial penetration welds. However, there may be some critical length and size dimensions of the incomplete penetration for which the blast performance of the welded panel is not adversely affected.